

*FERROMAGNETISM AND ANTIFERROMAGNETISM  
OF RARE-EARTH METALS*

K. P. BELOV, R. Z. LEVITIN, and S. A. NIKITIN

Usp. Fiz. Nauk 82, 449-498 (March, 1964)

CONTENTS

1. Magnetic Properties of Rare-earth Ferromagnets . . . . .	179
2. Neutron-Diffraction Studies of the Magnetic Structure of Rare-earth Ferromagnets . . . . .	183
3. Theory of the Helicoidal Magnetic Structure . . . . .	184
4. Nature of Magnetic Phase Transitions in Rare-earth Ferromagnets . . . . .	190
5. Antiferromagnetism of Metals of the Cerium Subgroup . . . . .	191
6. Magnetoelastic Properties of Rare-earth Ferromagnets . . . . .	193
7. Electrical and Galvanomagnetic Properties of Rare-earth Ferromagnets . . . . .	198
8. Magnetic Properties of Rare-earth Alloys . . . . .	202
Literature. . . . .	206

INVESTIGATIONS over the last few years have established that six rare-earth metals of the yttrium subgroup—Gd, Tb, Dy, Ho, Er, and Tm—have ferromagnetic properties. The rare-earth ferromagnets (r.e.f.) have very characteristic magnetic properties, different from those of ferromagnets of the iron group. The most remarkable property of r.e.f., which is at present arousing great interest, is the fact that five of them (Tb, Dy, Er, Ho, and Tm) exhibit antiferromagnetism in a certain range of temperatures. Investigations have shown that this antiferromagnetism is of a special type: spiral or helicoidal.\*

The majority of the rare-earth metals of the cerium subgroup (Ce, Nd, Sm, Eu) exhibit antiferromagnetism at very low temperatures.

A wealth of experimental data on the magnetic properties of rare-earth metals has been accumulated in recent years, and attention has also been focused on the theory of helicoidal antiferromagnetism. The present review is an attempt to present systematically this material.

1. MAGNETIC PROPERTIES OF RARE-EARTH FERROMAGNETS

The magnetic properties of dysprosium have been investigated in the greatest detail.<sup>[1-4]</sup> Figure 1, which is taken from <sup>[3]</sup>, illustrates the temperature dependence of the specific magnetization of a single crystal (of hexagonal symmetry) of dysprosium in the basal plane along the a-axis. The curves were recorded between helium temperatures and 300°K in various magnetic fields. Figure 1 shows that the magnetization rapidly decreased on reaching a certain tem-

perature; when the magnetic field is increased, this magnetization drop occurs at higher temperatures. In a field approaching zero, the magnetization drop occurred at  $\theta_1 = 85^\circ\text{K}$ . It follows from Fig. 1 that in the region of  $\theta_2 = 179^\circ\text{K}$  there is an increase of magnetization, followed by a decrease at higher temperatures.

The interpretation of the results of these measurements suggested at once that the ferromagnetic-antiferromagnetic transition occurs at  $\theta_1$  and the antiferromagnetic-paramagnetic transition at  $\theta_2$ , i.e., that dysprosium, in contrast to normal ferromagnets, exhibits two magnetic phase transitions.

Similar results were obtained for holmium<sup>[4,5,20]</sup> (Fig. 2), erbium<sup>[4,6,7]</sup> (Fig. 3), terbium<sup>[9]</sup> and thulium<sup>[5,10]</sup> (Fig. 4). In these metals, as in dysprosium, two transitions were observed: from the ferromagnetic to the antiferromagnetic state at  $\theta_1$ , and from the antiferromagnetic to the paramagnetic state at  $\theta_2$ .

The antiferromagnetism of r.e.f. can be "destroyed" by a magnetic field. At any given temperature, there is a critical field  $H_{\text{Cr}}$  at which this occurs. Figure 5 shows the isotherms of the magnetization of a dysprosium single crystal, and Fig. 6 presents the same data for holmium (in the basal plane along the a-axis). It is evident that, in the temperature region  $\theta_1 < T < \theta_2$ , in weak fields the magnetization increases linearly with the field, but at a certain critical field  $H_{\text{Cr}}$  the magnetization increases more sharply: the magnetic field produces a transition from the antiferromagnetic to the ferromagnetic state. The value of the critical field  $H_{\text{Cr}}$  increases approximately linearly with temperature, reaching a maximum close to  $\theta_2$  (Fig. 7).

Experiments have shown that the critical fields of dysprosium, holmium, erbium, and thulium attain considerable values:

$$H_{\text{Cr max}} \approx 10\,000\text{--}18\,000 \text{ Oe.}$$

\*The problem of the existence of helicoidal antiferromagnetism in the sixth r. e. f.—gadolinium—has not yet been finally solved.

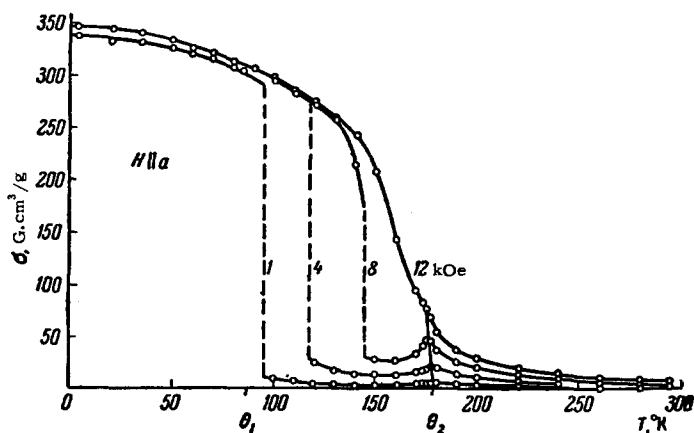


FIG. 1. Temperature dependence of the specific magnetization of a dysprosium single crystal in the basal plane (along the a-axis) in various fields.

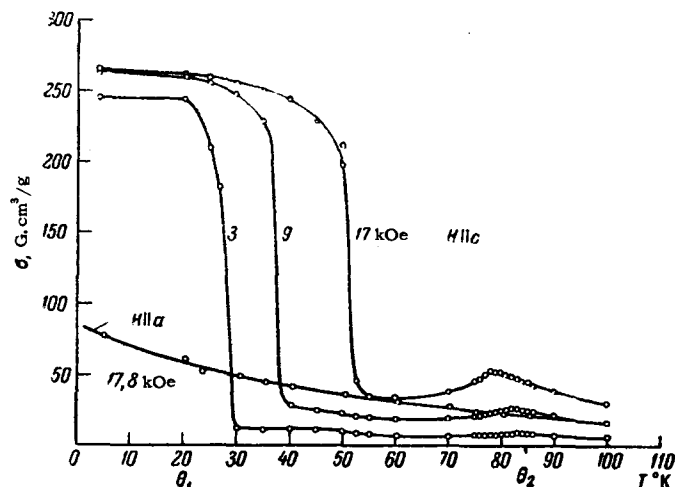


FIG. 3. Temperature dependence of the specific magnetization of an erbium single crystal along the hexagonal c-axis and the basal plane a-axis in various fields.

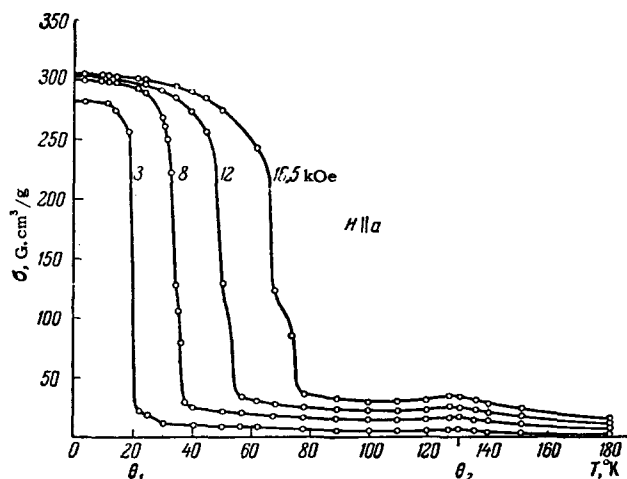


FIG. 2. Temperature dependence of the specific magnetization of a holmium single crystal in the basal plane along the a-axis in various fields.

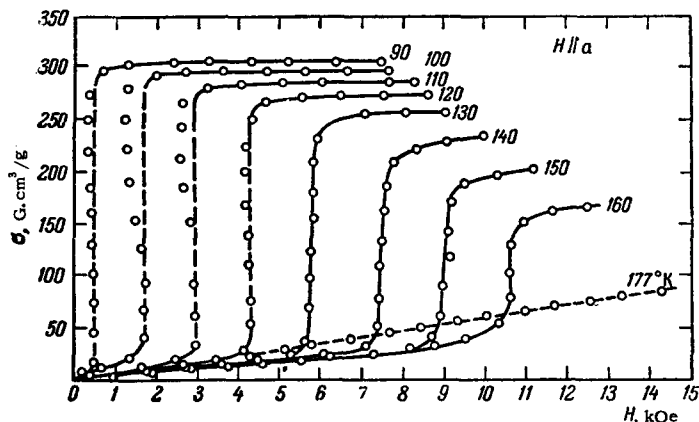


FIG. 5. Isotherms of the magnetization of a dysprosium single crystal in the basal plane along the a-axis.

In the case of terbium, the temperatures  $\theta_1$  and  $\theta_2$  lie very close to each other, and it is difficult to distinguish them in experiments. The values of  $\theta_1$  and  $\theta_2$  of terbium were determined by measuring the galvanomagnetic effect (magnetoresistance), which is

very sensitive to magnetic structure; at the transition points, clear maxima are obtained on the curves  $1/R(\Delta R/R)(T)$ .<sup>[2]</sup> The value of the critical field of terbium is two orders of magnitude lower ( $H_{cr,max} \approx 200$  Oe) than those of dysprosium, holmium, erbium, and thulium.

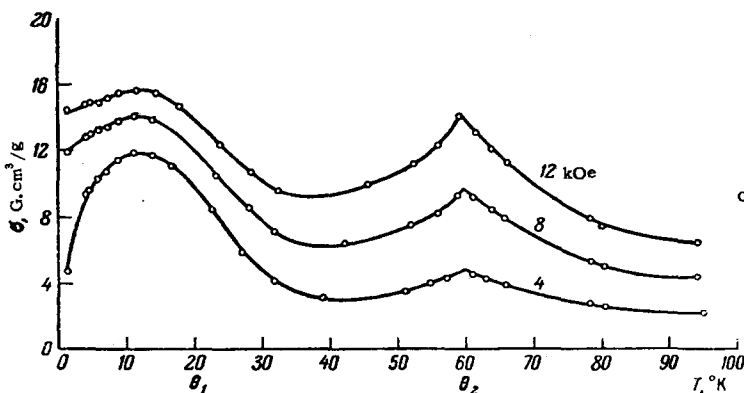


FIG. 4. Temperature dependence of the specific magnetization of polycrystalline thulium in various fields.

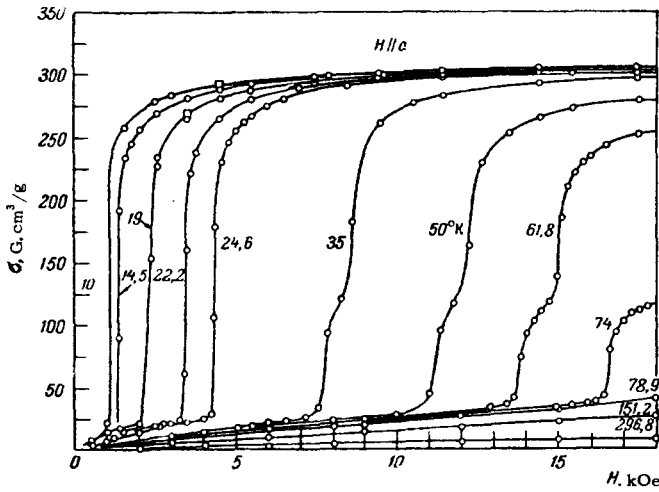


FIG. 6. Isotherms of the magnetization of a holmium single crystal in the basal plane along the a-axis.

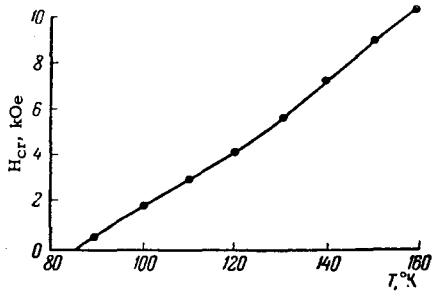


FIG. 7. Temperature dependence of the critical field  $H_{cr}$  of dysprosium.

Until very recently, gadolinium was regarded as a "normal" ferromagnet like iron, nickel and cobalt. [11,12] Recent measurements [13,14] have shown that in weak fields magnetization anomalies appear in the region 210–250°K; the magnetization decreases sharply on heating in this temperature range (Fig. 8). The magnetization isotherms (Fig. 9) above 210°K show critical-like fields (measurements were carried out on toroidal samples of polycrystalline gadolinium) whose values, as in the case of dysprosium, rise with increase of temperature. However, the value of  $H_{cr}$  of gadolinium is very low ( $H_{cr,max} = 10-15$  Oe). This probably explains why these anomalies were not discovered earlier in gadolinium: the previous work was carried out in strong fields using short samples.

In connection with this complex behavior of gadolinium, a suggestion has been put forward [13,14] that antiferromagnetism exists in this metal in the temperature range from 210–250 to 290°K, and is destroyed by a weak magnetic field. This suggestion was confirmed by the weaker intrinsic magnetization in gadolinium (Sec. 4) compared with the "normal" ferromagnets, and by the theoretical calculations of Kaplan and Lyons [49]. On the other hand, measurements on single crystals [15] did not show any change

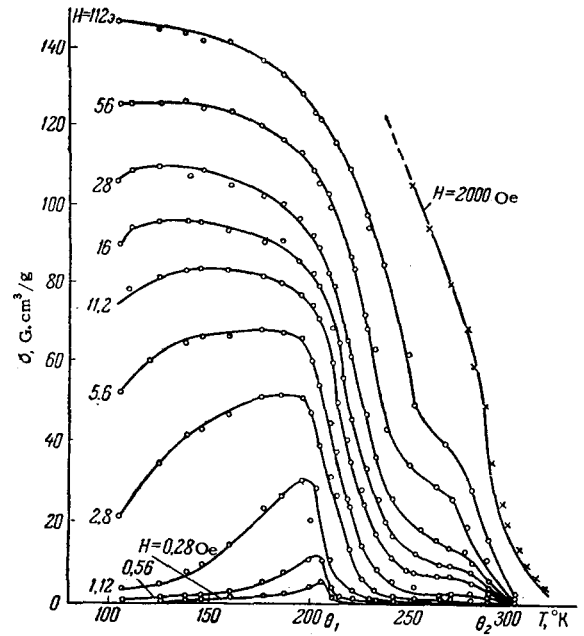


FIG. 8. Temperature dependence of the specific magnetization of polycrystalline gadolinium in various fields.

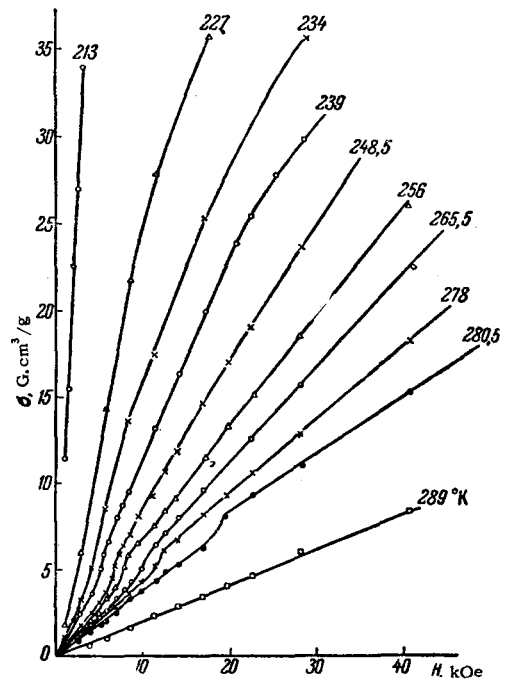


FIG. 9. Isotherms of the magnetization of polycrystalline gadolinium.

in the magnetic properties in the 210–290°K region. To give a final answer to the question of the existence and nature of antiferromagnetic ordering in gadolinium, further detailed studies of its magnetic structure are required.

Table I lists the values of  $\theta_1$ ,  $\theta_2$ , and  $H_{cr,max}$  for r.e.f.

Table I. Temperatures  $\theta_1$  and  $\theta_2$  and maximum critical

R. e. f.	$\theta_1$ , °K	$\theta_2$ , °K	$\theta_2 - \theta_1$ , °K	$H_{cr}$ max	Reference
Dy	85	179	94	11 000	3
Ho	20	133	113	18 000	4
Er	20	85	65	18 000	4
Tu	22	60	38	>15 000	5
Tb	219	230	11	200	17

There is great interest in the anisotropy of the magnetic properties of r.e.f., because the magnetic anisotropy energy affects considerably the magnetic structure of these substances. At low (nitrogen and helium) temperatures, the uniaxial magnetocrystalline anisotropy energy of all the r.e.f. considered is very high. This is clear even from the fact that at helium temperatures the magnetic saturation of polycrystalline samples of dysprosium, holmium, terbium, and thulium is not reached even in fields of 80 kOe.<sup>[15-20]</sup> The investigations of single crystals show that in some r.e.f. the easy magnetization axis lies in the basal plane (for example, in dysprosium<sup>[3,4]</sup>), while in others (for example, in erbium<sup>[7]</sup> and holmium<sup>[4]</sup>) it is directed at an angle to the hexagonal axis. In gadolinium crystals, the direction of the easy magnetization axis varies with temperature;<sup>[23,24]</sup> the angle between the easy magnetization axis and the hexagonal axis increases from 32 to 90° on increasing the temperature from 0 to 170°K (angle  $\theta$  in Fig. 10a). In the temperature range from 250°K to the Curie point (290°K), the easy magnetization axis coincides with the c-axis. This behavior is due to the complex temperature dependence of the uniaxial magnetic anisotropy constants  $K_1$  and  $K_2$  of gadolinium (Fig. 10b).

Investigations of dysprosium, erbium and holmium single crystals showed that a strong uniaxial anisotropy occurred also above the temperature  $\theta_2$  — in the paramagnetic region. This brought out the fact that the paramagnetic susceptibility and the paramagnetic Curie

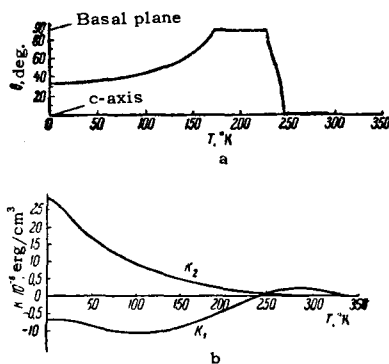


FIG. 10. a) Temperature dependence of the direction of easy magnetization of gadolinium (the angle  $\theta$  is reckoned from the hexagonal c-axis of the crystal); b) temperature dependence of the uniaxial anisotropy constants of gadolinium.

points vary with direction in the crystal.<sup>[3,4,21]</sup> Thus, for dysprosium the paramagnetic Curie point along the hexagonal axis is  $\theta_{p\parallel} = 121^\circ\text{K}$ , and in the basal plane it is  $\theta_{p\perp} = 169^\circ\text{K}$  ( $\Delta\theta_p = 48^\circ\text{K}$ ); for erbium, these quantities are, respectively, 61.7 and 32.5°K ( $\Delta\theta_p = 29.9^\circ\text{K}$ ); and for holmium, they are 73 and 88°K ( $\Delta\theta_p = 15^\circ\text{K}$ ).

From Landau's thermodynamic theory<sup>[25]</sup> it follows that in an antiferromagnet the ratio  $\Delta\theta_p/\theta_{p\parallel}$  is equal to the ratio of the magnetic anisotropy and exchange interaction energies. For dysprosium, this ratio is  $\Delta\theta_p/\theta_{p\parallel} = 0.27$ ; for erbium,  $\Delta\theta_p/\theta_p = 0.35$ ; and for holmium,  $\Delta\theta_p/\theta_p = 0.11$ . Thus, in these rare-earth metals, the uniaxial anisotropy energy is comparable with the exchange interaction energy. The strong uniaxial magnetocrystalline anisotropy of r.e.f. is due to the fact that they have close-packed hexagonal lattices.

We have considered so far the uniaxial anisotropy energy (the anisotropy of the second and fourth orders). It has been shown, however, that the energy of the magnetic anisotropy in the basal plane (the anisotropy of the sixth order) plays an important role in r.e.f. In dysprosium<sup>[3,4]</sup>, the latter energy is large at  $T < \theta_1$  (in the ferromagnetic state) and is retained in the antiferromagnetic region at  $T < 110^\circ\text{K}$ . Above 110°K, the basal-plane anisotropy is practically equal to zero.

It is of interest to study the hysteresis properties of r.e.f., particularly in the region between  $\theta_1$  and  $\theta_2$ . Figures 11 and 12 show the temperature dependences of the coercive force  $H_C$  of dysprosium<sup>[26]</sup> and gadolinium<sup>[13]</sup> (see also<sup>[27,28]</sup>). In dysprosium, the coercive force near  $\theta_1$  is relatively small, but on in-

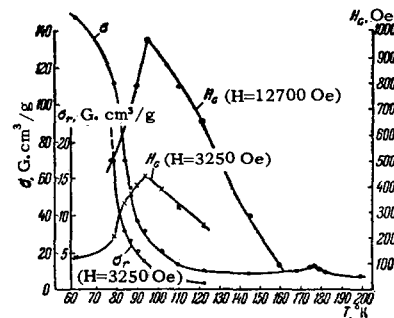


FIG. 11. Temperature dependence of the coercive force  $H_C$  and the remanent magnetization  $\sigma_2$  of dysprosium (for magnetization in fields of 3250 and 12 700 Oe).

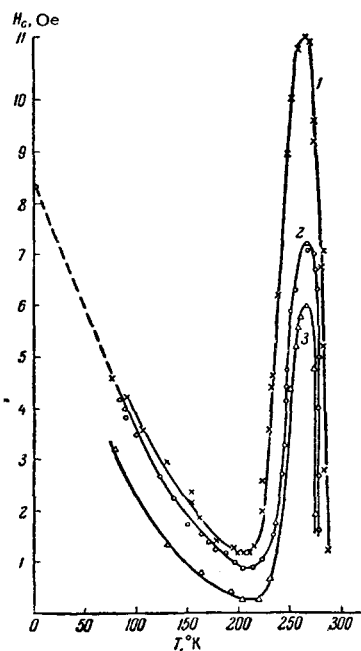


FIG. 12. Temperature dependence of the coercive force of gadolinium. 1) Unannealed gadolinium (99.5% purity); 2) unannealed gadolinium (99.8% purity); 3) annealed gadolinium (99.8% purity).

creasing the temperature above  $\theta_1$ , the coercive force increases strongly—reaching a maximum at 90–95°K—and then rapidly decreases. We may assume that the reason for this increase of  $H_c$  is the existence of an unusual magnetically heterogeneous state in the region above  $\theta_1$ : the ferromagnetic and antiferromagnetic phases coexist because the transition is broad. The coercive force maximum was also found at  $\theta_1$  in terbium.<sup>[26]</sup>

A sharp rise of the coercive force in gadolinium in the range 210–250°K is possibly due to the same reason.

## 2. NEUTRON-DIFFRACTION STUDIES OF THE MAGNETIC STRUCTURE OF RARE-EARTH FERROMAGNETS

A detailed neutron-diffraction study was recently carried out on single crystals of dysprosium, holmium,

erbium, terbium, and thulium. It was found that the magnetic moments are not collinear in these metals: they have either spiral (helical) or more complex—umbrella-shaped (cycloidal)—magnetic structures.

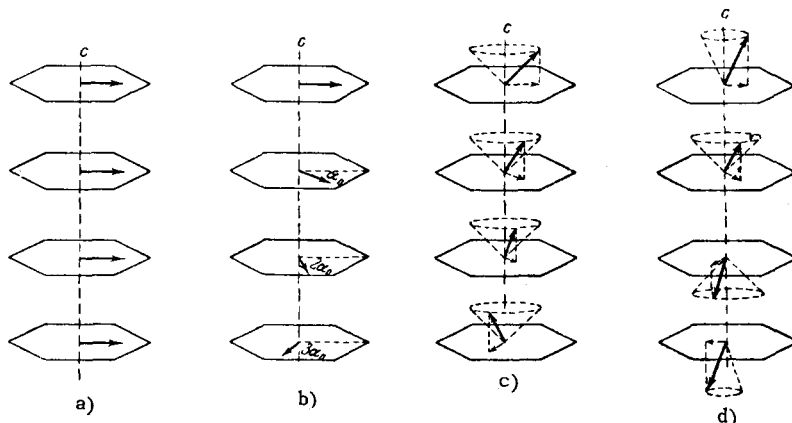
Dysprosium has the simplest magnetic structure.<sup>[29,30]</sup> In the ferromagnetic region, below the  $\theta_1$  point, the magnetic moments of dysprosium lie in the basal planes and are parallel to one another (Fig. 13a). In the antiferromagnetic state, in the temperature region between the points  $\theta_1$  and  $\theta_2$ , the resultant magnetic moment of each basal plane is rotated by a certain angle  $\alpha_0$  with respect to the direction of the moment in the next basal plane (Fig. 13b). It is evident from Fig. 13b that the magnetic moments in the hexagonal lattice of dysprosium lie on a spiral, the result of which is the characteristic “helical” structure. Neutron-diffraction studies of dysprosium established that the angle  $\alpha_0$  increases almost linearly from 26.5 to 43.2° with increase of temperature from  $\theta_1$  to  $\theta_2$ . In the temperature region below 140°K, the helical structure is slightly distorted, apparently because of the effect of the magnetic anisotropy in the basal plane.

The magnetic structure of terbium is similar to the magnetic structure of dysprosium.<sup>[31]</sup>

The magnetic structure of holmium is more complex.<sup>[30,32]</sup> Below the point  $\theta_1$  in the ferromagnetic state, the magnetic moment component along the hexagonal axis of holmium is (at 4.2°K)  $2\mu_B$  per atom. At the same temperature, the magnetic moment component in the basal plane is  $9.5\mu_B$  per atom; the magnetic field components in the basal plane are helicoidally ordered with the angle  $\alpha_0 = 36^\circ$  and do not have a resultant magnetic moment (Fig. 13c). Thus, the ferromagnetic moment of holmium below  $\theta_1$  is due only to the component parallel to the hexagonal axis. In the antiferromagnetic state, above 20°K but below 35°K, holmium has a strongly distorted helical structure with  $\alpha_0 = 36^\circ$ ; above the latter temperature, the purely helical ordering is observed and the helical angle  $\alpha_0$  increases linearly to 50° at the temperature  $\theta_2$ .

In the ferromagnetic state, erbium<sup>[30,33]</sup> has a structure similar to that of holmium below  $\theta_1$ : the magnetic moment component along the c-axis is (at 4.2°K)  $7.2\mu_B$  per atom, while the component in the

FIG. 13. Magnetic structures of r. e. f. a) Ferromagnetic structure of dysprosium—collinear ordering; b) antiferromagnetic structure of dysprosium, holmium, and terbium—antiferromagnetic helical; c) ferromagnetic structure of holmium and erbium—ferromagnetic helical; d) antiferromagnetic structure of erbium—cycloidal ordering.



basal plane, equal to  $4.1 \mu_B$  per atom, is ordered helicoidally with  $\alpha_0 = 43.3^\circ$ . In the antiferromagnetic region, the magnitude and direction of the magnetic moment component along the c-axis vary periodically from layer to layer in accordance with a sine law (Fig. 13d). The period of this variation is  $4c_0$  ( $c_0$  is the lattice constant along the c-axis) at  $T = 20^\circ\text{K}$ , and then it decreases linearly to  $3.5c_0$  when the temperature is increased to  $52^\circ\text{K}$ , remaining constant above this temperature. In the temperature range from  $\theta_1 = 20^\circ\text{K}$  to  $52^\circ\text{K}$ , the neutron-diffraction patterns show additional reflection maxima, obviously because the magnetic moment components in the basal plane are helicoidally ordered in this temperature region. Above the latter temperature, the components in the basal plane are disordered.

Thus, according to the neutron-diffraction data, erbium should exhibit an additional transition at  $52^\circ\text{K}$  from the ordered helicoidal to the disordered structure in the basal plane, as confirmed by measurements of the specific heat and electrical resistance of this metal.

Neutron-diffraction studies of polycrystalline thulium showed<sup>[30]</sup> that the magnetic structure of this metal in the antiferromagnetic region is similar to that of erbium. Recently, thulium single crystals were investigated by neutron diffraction.<sup>[34]</sup> Between  $39^\circ$  and  $56^\circ\text{K}$ , thulium has a structure similar to the high-temperature structure of erbium with a modulation period of  $3.5c_0$ . At  $4.2^\circ\text{K}$ , the resultant magnetic moment, equal to  $1 \mu_B$  per atom, is directed along the c-axis. In this temperature region, the spins alternate: in four neighboring planes the magnetic moments are directed one way, and in the three next planes they are directed in the opposite way.

The magnetic structure of gadolinium has not yet been studied since this metal absorbs neutrons strongly.

To conclude this section, we note that helicoidal magnetic structures are observed not only in rare-earth metals, but are found also in the alloy  $\text{MnAu}_2$ ,<sup>[35,36]</sup> in manganese dioxide  $\text{MnO}_2$ ,<sup>[37]</sup> in some compositions of the alloys  $\text{Mn}_{2-x}\text{Cr}_x\text{Sb}$ ,<sup>[38]</sup> in holmium iron garnet,<sup>[39]</sup> in manganese chromite,<sup>[40]</sup> and in the compound  $\text{MnI}_2$ .<sup>[41]</sup> There is some doubt about the interpretation of the magnetic structure of chromium.<sup>[42]</sup> Kaplan<sup>[43]</sup> came to the conclusion that chromium has a helicoidal magnetic structure.

We must point out that the problem of describing the magnetic symmetry in helicoidal magnetic substances, having a magnetic structure period which, in general, is not a multiple of the crystal lattice period, is quite complicated since the magnetic symmetry group is not then directly related to the crystal symmetry group. Recently, magnetic symmetry theory was extended to the helicoidal structures of rare-earth metals by Naish.<sup>[44]</sup>

### 3. THEORY OF THE HELICOIDAL MAGNETIC STRUCTURE

The first attempt to explain the magnetic properties of dysprosium was made by Néel,<sup>[45]</sup> according to whom the hexagonal lattice of dysprosium splits into two sublattices. In each of these sublattices, there is a strong positive exchange interaction which orients the magnetic moments in the sublattices to make them parallel, i.e., it produces the ferromagnetic state. However, the exchange interaction between sublattices is relatively weak and negative. This interaction produces, in the temperature region  $\theta_2 - \theta_1$ , the antiparallel orientation of the resultant magnetic moments of the sublattices, i.e., it produces the antiferromagnetic state. Cooling increases the effective field of the uniaxial magnetic anisotropy, which destroys the antiferromagnetic structure at the temperature  $\theta_1$ , making the magnetic moments of the sublattices parallel. The discovery of the helicoidal magnetic structures in r.e.f. showed that Néel's theory is unsatisfactory and posed the following problems: 1) to explain the existence of the helicoidal magnetic structure; 2) to explain the transition from the helicoidal antiferromagnetic state to the ferromagnetic state; and 3) to describe the behavior of the helicoidal structure under the action of a magnetic field, elastic stresses and temperature.

At present, there is no complete theory which would explain the appearance of the helicoidal magnetic structure. In all the work dealing with this problem, the appearance of the helicoidal spin configuration is explained by the "competition" of the positive interaction between the nearest atomic neighbors, and of the negative interaction between the next nearest neighbors, an allowance being made for the interaction between even more distant neighbors. The possibility of the formation, in principle, of the helicoidal magnetic structure in rare-earth metals follows from the indirect nature of the exchange interaction in them.<sup>[46]\*</sup> The indirect exchange interaction via conduction electrons is a long-range effect and depends in a complex way on the separation between atoms. This may make the exchange interaction between the nearest atoms comparable in magnitude and opposite in sign to the exchange interaction between atoms at greater distances from one another.

We give below a brief resume of the theoretical results arising out of the investigation of helicoidal magnetic structures.

Yoshimori<sup>[37]</sup> was the first to discuss the possibility of the formation of the helicoidal distribution of magnetic moments in an  $\text{MnO}_2$  crystal. He showed

\*A review of the present state of the theory of the electron structure and the exchange interaction in rare-earth metals is given in the paper of S. V. Vonsovskii and Yu. A. Izyumov [UFN 77, 377 and 78, 3 (1962) Soviet Phys. Uspekhi 5, 547 and 723 (1963)].

that such a structure may be formed by the exchange interaction between the first, second, and third nearest neighbors, and he calculated the initial magnetic susceptibility of the helicoidal structure. Yoshimori showed also that in  $\text{MnO}_2$  a more complex (cycloidal) spin configuration may exist, with the magnetic moment components in the basal plane being ordered helicoidally and the components along the  $c$ -axis being modulated; he indicated the possibility that the uniaxial magnetic anisotropy energy may affect this structure. Starting from similar assumptions, Cooper<sup>[47]</sup> came to the conclusion that in the body-centered cubic lattice of chromium the helicoidal structure has the lowest energy for a certain relationship between the exchange integrals of neighboring atoms.

Villain<sup>[48]</sup> investigated, in the molecular-field approximation the various magnetic-moment configurations which may appear in a magnetic material below the point of transition to the magnetically ordered state. He further showed that when the interaction between the second and third neighbors is strong the helicoidal structure is the most stable from the energy point of view.

Kaplan et al.<sup>[50]</sup> found, starting from the spin-wave theory, that, for a certain relationship of the exchange interactions between sublattices and in sublattices themselves, the spiral magnetic structure is the principal state in cubic and tetragonally distorted structures of spinel type.

Yoshida and Miwa<sup>[51]</sup>, having discussed on the same basis the interaction in the hexagonal lattice of rare-earth metals, came to the conclusion that the antiferromagnetic helicoidal structure is possible in this lattice when one allows for the interaction between the next-nearest neighbors and for the strong uniaxial magnetocrystalline anisotropy. In their later work<sup>[52]</sup>, these same authors allowed for the anisotropy energy in the basal plane and showed that, in this case, the formation of more complex spiral structures—ferromagnetic and cycloidal—is possible. Similar calculations were carried out by Kaplan et al.,<sup>[49,53]</sup> Elliott,<sup>[54]</sup> Herpin,<sup>[55]</sup> and Nagamiya et al.<sup>[56]</sup>

In all the cited papers, the formation of the helicoidal magnetic structure was explained, as previously mentioned, by the competition of the positive and negative exchange interactions. The exception to this rule was the work of Sato,<sup>[57]</sup> who suggested that the helicoidal structure of the alloy  $\text{MnAu}_2$  was due to the magnetodipole interaction. He was of the opinion that the interaction between the next-nearest neighbors was determined not by the exchange forces but by the magnetodipole forces since the latter decrease with distance much more slowly than do the exchange forces.

As already mentioned, the second theoretical problem is the explanation of the transition from ferromagnetism to helicoidal antiferromagnetism. The first attempt to provide an explanation was made by

Néel, as reported above. Although Néel's theory and its refinement by Liu et al.<sup>[58]</sup> starts from the two-sublattice model, Néel's idea that the transition from the ferromagnetic to antiferromagnetic state occurs under the influence of the magnetic anisotropy energy has been developed in later work.

The assumption of the influence of the magnetic anisotropy energy on the stability of the helicoidal magnetic structure of dysprosium and the allowance for this influence in explaining the transition from ferromagnetism to antiferromagnetism at the point  $\theta_1$  were made by Enz.<sup>[59]</sup> In his calculations, which were of a thermodynamic nature, Enz allowed (apart from the energy of the exchange interaction between the nearest and next-nearest layers) for the energy of the uniaxial magnetic anisotropy and of the magnetic anisotropy in the basal plane. However, he assumed that the point of transition from the helicoidal antiferromagnetic state to the ferromagnetic state is influenced chiefly by the nature of the temperature dependence of the integrals of the exchange between layers.

Yosida and Miwa, in their aforementioned work,<sup>[51,52]</sup> explained the transition in rare-earth metals from one magnetic structure to the other by the fact that the anisotropy constants of the second, fourth, and sixth orders vary in different ways with temperature. Thus, for example, the helicoidal magnetic structure of dysprosium appears due to the strong uniaxial anisotropy (the anisotropy of the second and fourth orders), which holds the magnetic moments in the basal plane. On cooling, the anisotropy energy in the basal plane (the anisotropy of the sixth order) increases. Consequently, at the temperature  $\theta_1$ , the helicoidal magnetic structure is destroyed and the energetically more stable ferromagnetic structure is established. It should be noted, however, that the temperature dependence of the helicoidal structure pitch, calculated by Yosida and Miwa, does not agree with the experimental data. Similar calculations were carried out by other workers.<sup>[53-56]</sup>

The transition from the ferromagnetic to antiferromagnetic state is explained in a different way in Kittel's thermodynamic theory.<sup>[60]</sup> He showed that the transition from the parallel to the antiparallel spin configuration in the compound  $\text{Mn}_{2-x}\text{Cr}_x\text{Sb}$  can be explained by assuming that the exchange integral changes sign at a certain critical value of the lattice parameter in consequence of a strong dependence of this exchange integral on the interatomic spacing. Kittel put forward his hypothesis for the transition from ferromagnetism to antiferromagnetism in the two-sublattice magnetic structure, but it deserves special discussion in the case of transition from the helicoidal antiferromagnetic to the ferromagnetic state (see p. 189 below).

Thus, the causes of the formation and destruction of the helicoidal magnetic structure and of the complex magnetic behavior of r.e.f. are still not clear.

Because of this, it is of great interest to compare the experimental data with the existing theory of helicoidal antiferromagnetism (according to Enz).

Enz<sup>[59]</sup> used in his theory the same assumptions which were made earlier by Herpin, Meriel, and Villain<sup>[61]</sup> to interpret the magnetic properties of the alloy MnAu<sub>2</sub>, which has a helicoidal magnetic structure. The basis of Enz's calculations is as follows. A hexagonal crystal, possessing uniaxial anisotropy due to which the magnetic moments lie in the basal plane, is considered. It is assumed that a strong positive exchange interaction, producing ferromagnetic ordering of the moments in the basal plane, acts between atoms lying in the same basal plane. An allowance is made both for the exchange interaction between atoms in the neighboring basal planes (exchange integral  $I_1$ ) and between atoms lying in alternate layers (exchange integral  $I_2$ ). It is then assumed that the exchange interaction between atoms in the neighboring planes is positive and that between atoms in the alternate planes is negative ( $I_1 > 0$ ,  $I_2 < 0$ ). The "competition" of the positive and negative exchange interactions rotates the magnetic moments in neighboring planes by an angle  $\alpha$ , and thus a helicoidal antiferromagnetic structure is formed.

The energy of the exchange interaction between layers can, in this case, be written as follows:\*

$$E_{exc} = -\mu_s^2 (I_1 \cos \alpha + I_2 \cos 2\alpha), \quad (1)$$

where  $\mu_s$  is the spontaneous magnetic moment per atom,  $\alpha$  is the angle between the magnetic moments in the first and second layers, and  $2\alpha$  is the angle between moments in the first and third layers. If we neglect other forms of energy (in particular, the magnetic anisotropy energy and the magnetoelastic energy in the basal plane), then the equilibrium value of the angle  $\alpha$  is found from the condition

$$\frac{\partial E_{exc}}{\partial \alpha} = 0. \quad (2)$$

Differentiating Eq. (1), we find

$$I_1 \sin \alpha_0 + 2I_2 \sin 2\alpha_0 = 0, \quad (3)$$

and hence the helicoidal angle is given by

$$\cos \alpha_0 = -\frac{I_1}{4I_2}. \quad (4)$$

Elementary calculations show that the helicoidal structure is stable under the condition

$$\frac{I_1}{|I_2|} \leq 4. \quad (5)$$

\*This expression follows from that generally accepted in the theory of ferromagnetism:

$$E_{exc} = -\sum 2I_{ij} S_i S_j \cos \psi_{ij},$$

where  $S_i$  and  $S_j$  are the spin moments of the neighboring atoms and  $\psi_{ij}$  is the angle between them.

If  $|I_2|$  is less than  $I_1/4$ , then the interaction between second-nearest neighbors is insufficient to form the helicoidal magnetic structure, and

$$\alpha_0 = 0. \quad (6)$$

In this case, we have the normal ferromagnetic ordering.

Herpin and Meriel<sup>[36]</sup> considered the behavior of the magnetic helicoidal structure in an external magnetic field directed at right-angles to the hexagonal axis of the crystal. On the application of this field, the angle between the direction of the magnetic moments in neighboring planes changes and depends on the orientation of these moments with respect to the field. The helicoidal structure energy in a magnetic field can be written in the form

$$E = -\mu_s^2 \sum_i [I_1 \cos (\theta_i - \theta_{i-1}) + I_2 \cos (\theta_i - \theta_{i-2})] - \mu_s H \sum_i \cos \theta_i. \quad (7)$$

Here,  $\theta_i$  is the angle between the field and magnetic moment directions in the  $i$ -th layer. The second term in Eq. (7) is the energy of the magnetic material in a magnetic field. If  $H = 0$ , then the angle between the directions of the magnetic moment of the  $i$ -th layer and of the field is

$$\theta_i = \theta_0 + i\alpha_0. \quad (8)$$

Herpin and Meriel<sup>[36]</sup> showed that in weak fields the helicoidal structure becomes somewhat deformed: the magnetic moments deviate from the perfect helicoidal distribution, becoming rotated by a certain angle toward the field (Fig. 14b). In this case, the magnetization  $m$  of a helicoidal antiferromagnet depends linearly on  $H$ :

$$m = \chi H, \quad (9)$$

where the susceptibility  $\chi$  is

$$\chi = -\frac{1}{32I_2} \frac{1}{\sin^4 \frac{\alpha_0}{2} [1 + 2 \cos \alpha_0 (1 + \cos \alpha_0)]}, \quad (10)$$

and the helicoid energy is given by the expression

$$E_{H < H_{cr}} = -\mu_s^2 (I_1 \cos \alpha_0 + I_2 \cos 2\alpha_0) - \frac{\chi H^2}{2}. \quad (11)$$

On increasing the magnetic field intensity, the helicoidal structure becomes energetically unstable and is destroyed by  $H = H_{cr}$ ; then the magnetization suddenly increases. The value of  $H_{cr}$  is<sup>[36]</sup>

$$H_{cr} = -7.76 \mu_s I_2 \sin^4 \frac{\alpha_0}{2}. \quad (12)$$

When  $H > H_{cr}$ , a pseudo-ferromagnetic structure is established: due to the action of the negative exchange interaction between alternate layers, the magnetic moments are not aligned strictly along the field but diverge slightly from the field direction (Fig. 14c). The magnetization in this range of fields is

$$m_0 = \mu_s - \frac{\mu_s (H_0 - H)}{\frac{H_0}{2} [2 + (1 + 2 \cos \alpha_0)^2]}. \quad (13)$$



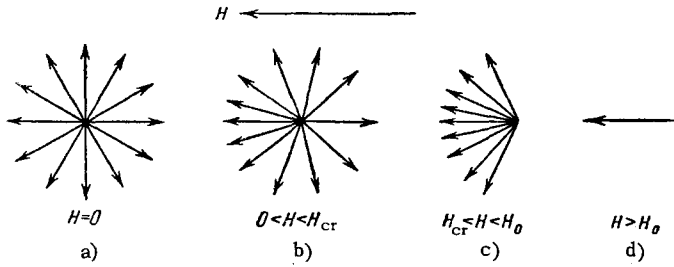


FIG. 14. Effect of a magnetic field on the helicoidal structure.

Here,  $H_0$  is the limiting field at which the deviations of the magnetic moments from the field direction are finally suppressed and the ferromagnetic ordering is established (Fig. 14d). This field is

$$H_0 = -16\mu_s I_2 \sin^4 \frac{\alpha_0}{2} = \frac{H_{cr}}{0.485}. \quad (14)$$

The energy of a helicoidal antiferromagnet in  $H_{cr} < H < H_0$  is given by the expression

$$E_{H_{cr} < H < H_0} = -\mu_s^2 (I_1 + I_2) - \mu_s H - \frac{\mu_s H_0}{2 + (1 + 2\cos \alpha_0)^2} \left(1 - \frac{H}{H_0}\right)^2. \quad (15)$$

Using the above formulas, we can calculate the magnetization curves of dysprosium and holmium from the experimental values of the critical field and saturation magnetization, taken from [3,4], and values of the angle  $\alpha_0$  taken from [29,32]. The calculated and experimental dependences  $\sigma(H)$  are given in Fig. 15

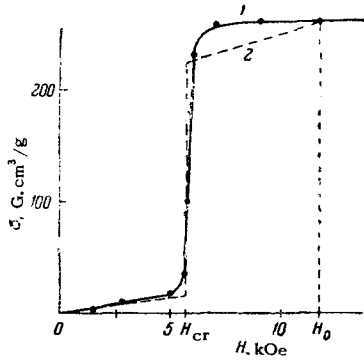


FIG. 15. Experimental (1) and theoretical (2) isotherms of the magnetization of a dysprosium single crystal in the basal plane ( $T = 130^\circ\text{K}$ ).

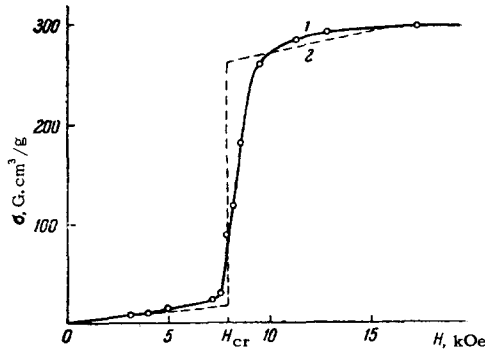


FIG. 16. Experimental (1) and theoretical (2) isotherms of the magnetization of a holmium single crystal in the basal plane ( $T = 35^\circ\text{K}$ ).

for dysprosium (at  $T = 130^\circ\text{K}$ ) and in Fig. 16 for holmium (at  $T = 35^\circ\text{K}$ ). It is evident that in both cases quite good agreement between the theoretical and experimental curves is obtained, but there is a discrepancy in the region  $H > H_{cr}$ .

It is known that above  $110^\circ\text{K}$  the magnetic anisotropy and basal-plane magnetostriction of dysprosium are small. Obviously, the magnetic anisotropy energy and the magnetoelastic energy do not influence greatly the helicoidal structure of holmium above  $35^\circ\text{K}$  either. For temperatures above  $110^\circ\text{K}$  in the case of dysprosium, and  $35^\circ\text{K}$  in the case of holmium, we can—using formulas (4) and (12), neutron-diffraction data, [29,32] and data from magnetic measurements [3,4]—calculate the exchange interaction integrals  $I_1$  and  $I_2$  as a function of temperature. These integrals are given for dysprosium in Fig. 17, and for holmium in Fig. 18.

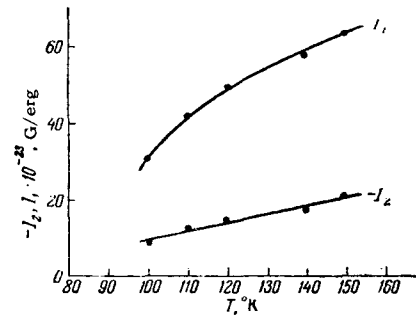


FIG. 17. Temperature dependence of the exchange integrals  $I_1$  and  $I_2$  for dysprosium.

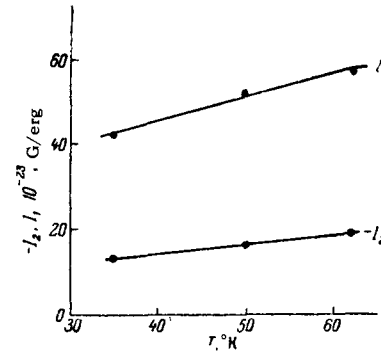


FIG. 18. Temperature dependence of the exchange integrals  $I_1$  and  $I_2$  for holmium.

For dysprosium, the maximum value of the energy of the exchange interaction between nearest layers (calculated per atom)

$$E_1 = \mu_s^2 I_1 \cos \alpha = 2.3 \cdot 10^{-14} \text{ erg},$$

and between alternate layers,

$$E_2 = \mu_s^2 I_2 \cos 2\alpha = 0.4 \cdot 10^{-14} \text{ erg}.$$

These values are comparable in their order of magnitude with the exchange interaction energy within a layer,  $E$ , which can be estimated from the value of

the temperature  $\theta_2$ . For dysprosium,  $E = k\theta_2 = 2.5 \times 10^{-14}$  erg. The quantities  $E_1$ ,  $E_2$  and  $E$  of holmium have approximately the same orders of magnitude.

As already mentioned, there is at present no agreed point of view on the nature of the interaction between the magnetic moments of layers which gives rise to the helicoidal magnetic structure. This interaction may, in general, be due not only the exchange interaction but also the magnetic dipole interaction.<sup>[57]</sup> However, the magnitude of the magnetic dipole interaction between layers is found to be two orders of magnitude smaller than that just calculated. The energy of the interaction of two magnetic dipoles is

$$E_{\text{dip}} \approx \frac{\mu_s^2}{r^3}. \quad (16)$$

Thus, the dipole-dipole interaction may be estimated by substituting into the above formula the values of the atomic magnetic moment and the distance between layers. In dysprosium the interactions between neighboring layers and between alternate layers are given by, respectively,  $4.5 \times 10^{-16}$  and  $0.56 \times 10^{-16}$  erg, i.e., values two orders of magnitude smaller than  $E_1$  and  $E_2$ . This allows us to conclude that the energy of the interaction between layers is really electrostatic in nature. The relatively large energy of the exchange interaction between alternate layers indicates the long-range nature of the exchange forces in dysprosium. This result is in agreement with the theoretical<sup>[46]</sup> and experimental<sup>[62]</sup> work on the long-range nature of the exchange interaction via conduction electrons.

Also of great interest is the fact that in the case of dysprosium and holmium the exchange interaction integrals depend quite strongly on temperature (Figs. 17 and 18). In the majority of the current theories, it is assumed that the value of the exchange integral varies little with temperature. Therefore, one might be satisfied with the statement that such a dependence as in the case of dysprosium and holmium indicates that the Enz-Herpin-Meriel theory, from which these parameters were calculated, is unsatisfactory. It is necessary, however, to point out that irrespective of the various theoretical assumptions the temperature dependence of the effective interaction between atomic planes in rare-earth metals follows directly from the experimental fact that the helicoid angle varies with temperature. In the majority of theoretical papers,<sup>[51-56]</sup> this is ascribed to the influence on the helicoidal structure of the anisotropy energy in the basal plane. However, de Gennes<sup>[46]</sup> showed that the influence of the anisotropy energy cannot explain the observed temperature dependence of the helicoid pitch. First, these dependences are observed near the transition  $\theta_2$ , i.e., where the anisotropy in the basal plane is weak. Secondly, the presence of the basal-plane anisotropy should distort the helicoidal structure, which was not observed in dysprosium above 110°K, and in holmium above 35°K, although above these tem-

peratures the variation of the helicoid angle with temperature is considerable. De Gennes<sup>[46]</sup> suggested the following qualitative explanation of the observed temperature dependence of the helicoid angle  $\alpha_0$ . The indirect exchange interaction via conduction electrons depends on the mean free path of electrons and therefore it may vary with temperature since this path is strongly temperature dependent.

The theories of Kittel,<sup>[60]</sup> and Been and Rodbell,<sup>[63]</sup> explaining the temperature dependence of the exchange interaction integral by its strong dependence on the crystal lattice parameter, are worth considering—especially in the case of rare-earth metals. We shall discuss this point in some detail.

Banister, Legvold, and Spedding<sup>[64]</sup> established that the parameter  $c_0$  of the hexagonal lattice of dysprosium (i.e., the distance between the basal planes) increases anomalously on cooling below  $\theta_2$ , while the parameter  $a_0$  (the distance between atoms within a basal plane) decreases weakly on cooling without exhibiting any singularities below  $\theta_1$  (Fig. 19). In other words, the thermal expansion anomaly due to the magnetic ordering is considerably greater along the c-axis than in the basal plane. It is natural to assume that the integral of the exchange interaction between layers in dysprosium depends on the distance between the basal planes.

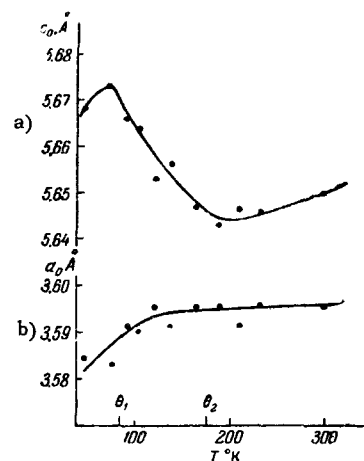


FIG. 19. Temperature dependence of the crystal lattice parameters  $c_0$  and  $a_0$  of dysprosium.

Figure 20 shows the dependence of  $I_1$  and  $I_2$  of dysprosium on the lattice parameter  $c_0$ . It is seen that, in the first approximation, the absolute values of  $I_1$  and  $I_2$  decrease when the lattice parameter is increased. Thus, within the framework of the Enz-Herpin-Meriel theory, the anomalous temperature dependence of the exchange integrals  $I_1$  and  $I_2$  of dysprosium can, according to Kittel and Been, be explained by the strong dependence of these integrals on the distance between the basal planes in hexagonal crystals of rare-earth metals. However, this conclusion is only hypothetical and requires experimental checking and theoretical justification.

We shall consider now the problem of the influence

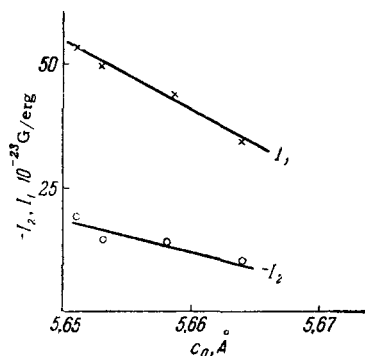


FIG. 20. Dependence of the integrals  $I_1$  and  $I_2$  of dysprosium on the lattice parameter  $c_0$ .

of the magnetic anisotropy forces on the transition temperature  $\theta_1$ . In the majority of papers, the transition from the helicoidal state to the ferromagnetic state is related to the increase of the anisotropy and magnetoelastic energies in the basal plane. The magnetic forces tend to orient the magnetic moments parallel to one another, favoring the destruction of the helicoidal structure.

The influence of the anisotropy and magnetoelastic energies in the basal plane on the transition temperature follows also from the approximate theory of Enz. Figures 21 and 22 show the temperature dependences of the ratio of the exchange integrals  $I_1/|I_2|$  for dysprosium and holmium, which represent the stability of the helicoidal magnetic structure [cf. Eq. (5)]. It is evident that on cooling this ratio increases, approaching the stability limit  $I_1/|I_2| = 4$ . However, extrapolation shows that when only the exchange interactions are allowed for, the helicoidal magnetic structure should be stable to  $50^\circ$  in dysprosium, and to  $0^\circ\text{K}$  in holmium. In fact, the transition temperatures  $\theta_1$  are  $85^\circ$  for dysprosium and  $20^\circ\text{K}$  for holmium. The difference is explained by the influence of the magnetic anisotropy energy and magnetoelastic energies in the basal plane.

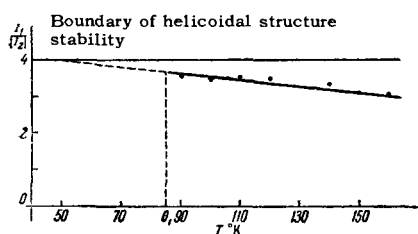


FIG. 21. Temperature dependence of the helicoidal structure stability for dysprosium.

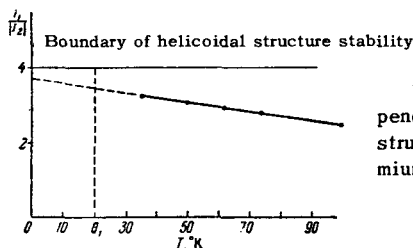


FIG. 22. Temperature dependence of the helicoidal structure stability for holmium.

We shall estimate the influence of the magnetic anisotropy and magnetoelastic energies in the basal plane on the helicoidal structure of dysprosium, for which these quantities are known. As previously stated, the magnetic anisotropy in the basal plane of dysprosium increases strongly at  $T \leq 110^\circ\text{K}$ . Thus, at  $100^\circ\text{K}$ , the saturation in the hard magnetization direction in the basal plane is reached in a field  $H_S = 7500$  Oe. This field is related to the anisotropy constant in the basal plane by the relationship<sup>[59]</sup>

$$H_s = \frac{36K}{M_s}.$$

Hence, we find the value  $K \approx 5 \times 10^5$  erg/cm<sup>3</sup>. Enz<sup>[59]</sup> used purely thermodynamic considerations to show, on the basis of the theory of phase transitions of the first kind, that in the presence of the anisotropy and magnetoelastic energies in the basal plane the critical field which destroys the helicoidal structure is

$$H_{cr} = H_{cr}^0 - \left( \frac{K}{M_s} + \frac{\lambda^2 E}{M_s} \right). \quad (16')$$

Here,  $H_{cr}^0$  is the critical field which, in the absence of the anisotropy and magnetoelastic energies in the basal plane, represents the effective exchange interaction between layers;

$$-\left( \frac{K}{M_s} + \frac{\lambda^2 E}{M_s} \right)$$

is the effective field of the magnetic anisotropy and magnetoelastic energies in the basal plane;  $\lambda$  is the magnetostriction constant;  $E$  is the elastic modulus; and  $M_s$  is the saturation magnetization. Substituting into Eq. (16') the values of  $K$  and  $M_s$ , we find that the effective magnetic anisotropy field in dysprosium at  $100^\circ\text{K}$  is approximately 200 Oe. The critical field at this temperature is  $H_{cr} = 1800$  Oe. Thus, already at this temperature the anisotropy has a considerable influence on the value of the critical field, tending to destroy the helicoidal distribution of the magnetic moments in dysprosium. On cooling, the influence of the effective anisotropy field increases even more because the anisotropy constant becomes larger (saturation in the hard direction is reached in fields  $H_S > 8000$  Oe). Moreover, it is necessary to allow for the influence of the magnetoelastic energy in the basal plane. Belov et al.<sup>[13]</sup> showed that the magnetostriction of dysprosium in the basal plane near the transition point  $\theta_1$  is unusually large (cf. Sec. 6). It has a value of the order of  $10^{-3}$  in fields of 15,000 Oe, which are still far from saturation. An estimate gives about 300 Oe for the value of the effective field of the magnetoelastic energy in the basal plane at  $85^\circ\text{K}$ , i.e., the magnetoelastic energy in the basal plane is comparable with the magnetic anisotropy energy and should also affect considerably the transition temperature  $\theta_1$  of dysprosium.

Thus we may conclude that in dysprosium (and obviously in other r.e.f.) the magnetic forces exert a considerable influence on the temperature of transition

from ferromagnetism to helicoidal antiferromagnetism.

From this comparison of theory with experimental data, it is evident that at present we cannot draw final conclusions about the causes of the formation in r.e.f. of the helicoidal antiferromagnetic structure. In particular, the question of the temperature dependence of the integrals of the exchange interaction between layers and of the nature of this dependence still remains open. To solve this problem, it is necessary to develop a rigorous quantum-mechanical theory of the magnetic ordering in r.e.f.

#### 4. NATURE OF MAGNETIC PHASE TRANSITIONS IN RARE-EARTH FERROMAGNETS

If the helicoidal magnetic structure were affected only by the exchange interaction forces between layers, the transition from the antiferromagnetic helicoidal state to the ferromagnetic state would be a phase transition of the second kind. The helicoidal magnetic ordering parameter (we can take the angle  $\alpha_0$  between the directions of the magnetic moments in neighboring planes as this parameter) should decrease smoothly on cooling, and at  $T = \theta_1$  the angle  $\alpha_0$  should become zero.

The transition at the point  $\theta_1$  is different in the presence of an effective field of the anisotropy and of the magnetoelastic energies in the basal plane. Below the point  $\theta_1$ , in the ferromagnetic region,  $\alpha_0 = 0$ ; on transition to the helicoidal magnetic structure, at the point  $\theta_1$ , the angle  $\alpha_0$  changes discontinuously. Thus, the presence of an effective field of the anisotropy energy and of the magnetoelastic energy in the basal plane makes the transition from the ferromagnetic to helicoidal antiferromagnetic state a magnetic phase transition of the first kind.

Measurements of the specific heat of r.e.f. [67-70] confirm this point of view. Figure 23 shows the temperature dependences of the specific heat for several r.e.f. It is seen that at the transition points  $\theta_1$  of dysprosium, erbium and holmium, symmetrical peaks

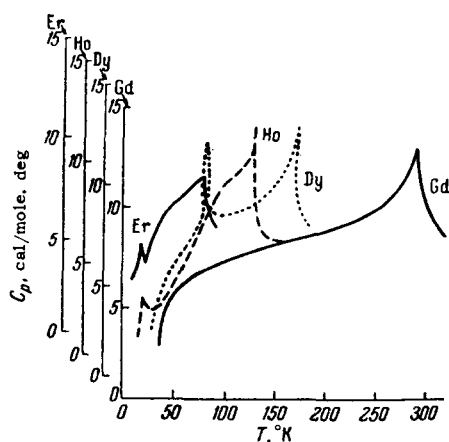


FIG. 23. Temperature dependence of the specific heat of rare-earth metals.

of the specific heat, characteristic of phase transitions of the first kind, are observed. Thermal hysteresis of the specific-heat peaks at the point  $\theta_1$  was also reported. [65] It must be pointed out that for the majority of r.e.f. the specific-heat peak at  $\theta_1$  is small compared with the peak at the point  $\theta_2$  (cf. Fig. 23), while for other rare-earth metals (gadolinium, thulium) it is altogether insignificant. This is because at the point  $\theta_1$  there is a transition from one type of magnetic ordering to another, while at  $\theta_2$  the magnetic order is destroyed. The energy of the former transition is relatively small and comparable with the magnetic anisotropy energy in the basal plane, whereas at the point  $\theta_2$  the exchange interaction energy in the basal plane must be overcome. Erbium also exhibits [67] an additional specific-heat peak at 53.5°K (barely discernible in Fig. 23), related to the ordering of the magnetic moment components in the basal plane (cf. Sec. 2).

The following observations must be made about the transition from the helicoidal antiferromagnetic state to the paramagnetic state at the point  $\theta_2$ .

1. In the case of dysprosium, holmium, erbium, and thulium this transition exhibits the characteristic features of the Néel point. Above all, this is indicated by the fact that the maxima of the temperature dependences of the susceptibility (or the magnetization) of these metals are shifted, as in typical antiferromagnets, toward low temperatures as the magnetic field is increased because the field "aids" the destruction of the antiferromagnetic ordering. Figure 24 shows such a shift of the point  $\theta_2$  under the action of a field on a single crystal of dysprosium. [3] Similar displacements of the  $\theta_2$  transition are observed for holmium, erbium, and thulium. It should be noted, however, that the transition at  $\theta_1$  is a "mixed" transition since at this point the ferromagnetic structure in the basal plane is destroyed simultaneously with the antiferromagnetic helicoidal structure. However, because the "helicoidal" energy of these metals is large, the nature of the transition is determined by the antiferromagnetic interaction between layers.

2. In terbium, the point  $\theta_2$  resembles the Curie point of normal ferromagnets since the "helicoidal"

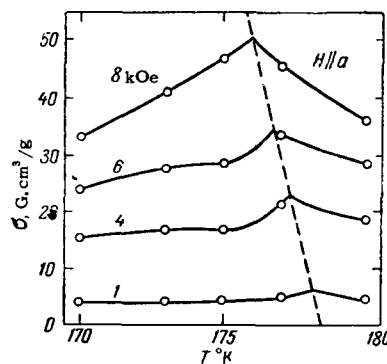


FIG. 24. Displacement of the transition temperature  $\theta_2$  of a dysprosium single crystal under the action of a magnetic field.

energy of this metal is much smaller than that of dysprosium. Therefore, here the ferromagnetic interaction in the basal planes plays the dominant role. If it is assumed that gadolinium also has the antiferromagnetic structure, then the remarks made about terbium apply also to gadolinium. The presence of the negative exchange interaction manifests itself in the value of the intrinsic susceptibility of gadolinium and terbium near  $\theta_2$ , being lower than that for normal ferromagnets. The magnitude of the intrinsic domain magnetization can be estimated from the intrinsic magnetization curve at the point of the transition to the paramagnetic state ( $\theta_2$ ). Magnetic measurements<sup>[13,26]</sup> (Fig. 25) showed that at the point  $\theta_2$  the magnetization of gadolinium and terbium varies with the field in accordance with the same law as the magnetization of normal ferromagnets (nickel and iron) at the Curie point:

$$\sigma_i = aH^{1/3}. \quad (17)$$

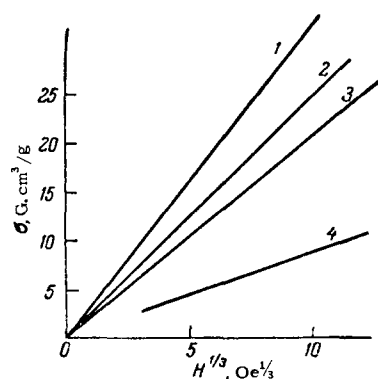


FIG. 25. Dependence of the intrinsic magnetization on  $H^{1/3}$ , measured in the region of the transition temperature  $\theta_2$ . 1) Tb; 2) Fe; 3) Gd; 4) Ni.

Belov<sup>[71]</sup> showed that for a normal ferromagnet the value of the coefficient  $a$  is proportional to  $\sigma_0/\theta^{1/3}$ , where  $\sigma_0$  is the specific saturation magnetization at  $0^\circ\text{K}$ . Since the values of  $\sigma_0$  of gadolinium and terbium are considerably higher than those of iron and nickel, the intrinsic susceptibility of these two rare-earth metals should be considerably greater than that of iron and nickel (the quantity  $\theta^{1/3}$  varies little from one ferromagnet to another).

However, the experimental values of the intrinsic susceptibility of gadolinium and terbium are small (the coefficient  $a$  is small), comparable with the value for iron. This is explained by the effect of the negative exchange interaction between layers, which prevents the magnetic moment from increasing on application of the field. This is also indicated by the smaller (compared with iron and nickel) magneto-caloric effect in gadolinium.<sup>[13]</sup>

## 5. ANTIFERROMAGNETISM OF METALS OF THE CERIUM SUBGROUP

The magnetic properties of the rare-earth metals of the cerium subgroup have been studied much less

than the metals of the yttrium subgroup because at present it is difficult to prepare sufficiently pure samples of the cerium subgroup metals; the presence of impurities distorts the results of magnetic measurements. Therefore, the data reported below should be regarded as preliminary.

**Lanthanum.** Measurements of the susceptibility<sup>[72]</sup> showed that lanthanum is a normal paramagnet.

**Cerium.** The face-centered cubic lattice of cerium undergoes a transition at low temperatures (or high pressures) into another cubic lattice but compressed so that its volume is reduced by 8%. Later investigations showed that, in addition to the "compressed" face-centered structure, at low temperatures there is also a phase with the close-packed hexagonal structure.<sup>[73]</sup> Neutron-diffraction experiments showed<sup>[74]</sup> that the transition to the "compressed" lattice is an electronic transition in which the magnetic 4f-electron goes over to the 5d-level in the conduction band; at the same time, cerium changes its valence from +3 to +4. Thus, in the high-temperature phase, as well as in the hexagonal structure, there is one magnetic electron in the 4f-state, while in the "compressed" cubic structure the 4f-shell is magnetically neutral. This complex behavior of the electron structure of cerium governs its complex magnetic behavior.<sup>[72,8,75]</sup> Figure 26 shows the temperature dependence of the reciprocal of the magnetic susceptibility of cerium. It is evident that the susceptibility depends on the number of cooling-heating cycles between room temperature and  $4.2^\circ\text{K}$ , increasing as the number of such cycles is increased. This effect is due to the fact that repeated cooling-heating cycles reduce the amount of the "compressed" face-centered phase (which does not have a magnetic moment) and increases the amount of the magnetic hexagonal phase. A maximum of the susceptibility, indicating a transition to the antiferromagnetic state, is found at  $12.5^\circ\text{K}$ . Similar results were obtained in measurements of the specific heat of Ce.<sup>[77,78]</sup>

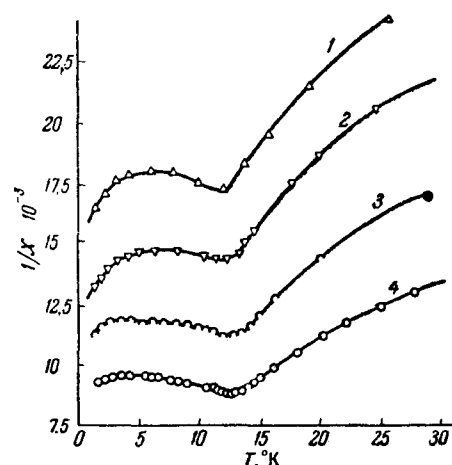


FIG. 26. Temperature dependence of the reciprocal of the susceptibility of cerium. 1) First cooling cycle from room temperature; 2) second cycle; 3) tenth cycle; 4) hundred-and-first and hundred-and-second cycles.

A specific-heat peak was observed in the region of 12°K (Fig. 27); the magnitude of this peak rose when the number of heating-cooling cycles was increased. Neutron-diffraction investigations<sup>[73]</sup> showed that at 4.2°K the hexagonal cerium has antiferromagnetic ordering with the magnetic moment directed along the c-axis, but it was not possible to determine the antiferromagnetic structure. The most probable value of the magnetic moment per cerium atom is, according to the neutron-diffraction data,  $0.6 \mu_B$ . This is considerably less than the magnetic moment of cerium ions in the  $^2F_{5/2}$ -state, which is  $2.17 \mu_B$  per atom. The difference is obviously due to the effect of the crystal field on the electron structure of cerium.

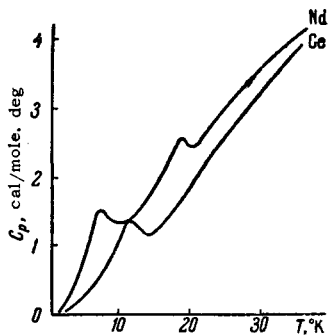


FIG. 27. Temperature dependence of the specific heat of cerium and neodymium.

Investigations of the electrical resistance of cerium were reported in<sup>[78,79]</sup>; a discontinuity, due to antiferromagnetic ordering, was found in the resistance curve at 12°K. The absence of such a discontinuity for other samples of cerium was due to the lower amount of the hexagonal phase.

**Praseodymium.** According to the results of magnetic measurements, praseodymium is a paramagnet.<sup>[72,80]</sup> Investigations of the specific heat<sup>[77]</sup> showed that a broad specific-heat maximum occurred in the region 60–100°K. In the same temperature region, the electric resistance is anomalous.<sup>[81]</sup> Lock<sup>[72]</sup> explained this behavior by a change of the electron structure of the metal at these temperatures.

**Neodymium.** At 7.5°K, the magnetic susceptibility of neodymium passes through a maximum<sup>[8,72,82]</sup> and therefore it has been concluded that neodymium is antiferromagnetic below this temperature. However, the behavior of the specific heat of neodymium<sup>[76]</sup> indicates the presence of another transition at 19°K; the temperature dependence of the specific heat exhibits a sharp maximum not only at 7.5°K but also at 19°K (cf. Fig. 27). The occurrence of two transitions in neodymium is indicated also by the behavior of the electrical resistance of this metal when the temperature is varied.<sup>[81]</sup> The nature of the transition at 19°K is still not clear.

Henry<sup>[17,20]</sup> investigated the magnetization of neodymium at low temperatures in fields up to 70,000 Oe. He found that the magnetization per atom at 1.3°K amounted to  $1.65 \mu_B$ . The difference between this

value and the theoretical value of  $3.27 \mu_B$  for the  $^4I_{9/2}$  state is explained by the influence of the crystal field on the electron structure of neodymium.

**Samarium.** Investigations of the magnetic susceptibility of polycrystalline samples of samarium<sup>[72,80]</sup> showed that below 15°K this metal undergoes a transition to the antiferromagnetic state: the susceptibility passes through a maximum at this temperature. A specific-heat maximum<sup>[83,84]</sup> and an electrical resistance anomaly<sup>[81]</sup> occur at the same temperature (Fig. 28). The same workers<sup>[81,84]</sup> showed also that, in addition to the specific-heat and electrical resistance anomalies at 15°K, there are also anomalies of these properties at 106°K although the magnetic susceptibility varies monotonically at the latter temperature. Because of this, Nesbitt et al.<sup>[122]</sup> suggested that the magnetic properties of samarium (and of other rare-earth metals of the cerium subgroup) are very sensitive to very small amounts of impurities and that investigations of purer samples are needed to establish the nature of the anomalies observed at 106°K.

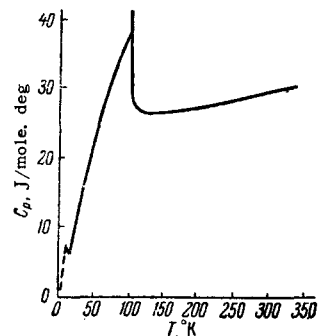
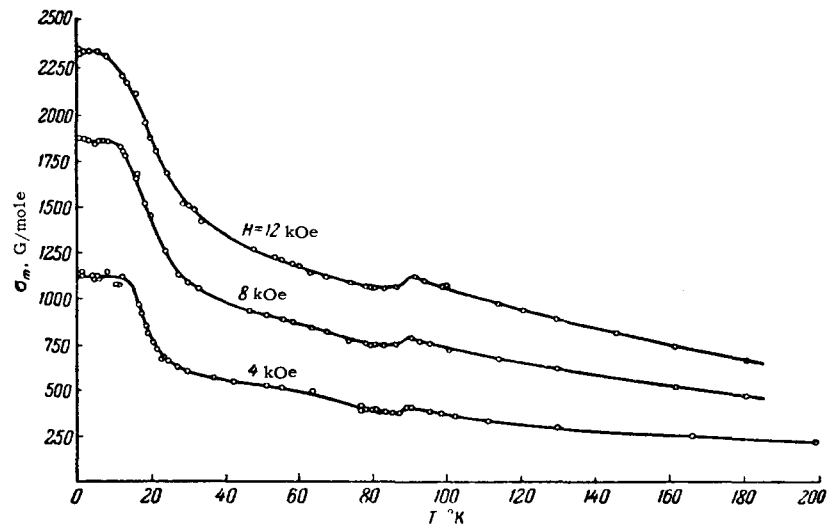


FIG. 28. Temperature dependence of the specific heat of samarium.

**Europium.** The magnetic susceptibility of europium increases strongly below 100°K and depends on the field.<sup>[85]</sup> From this, it has been concluded that europium becomes ferromagnetic below this temperature. However, later studies carried out by Bozorth and Van Vleck<sup>[86]</sup> have shown that below 90°K europium becomes antiferromagnetic. The susceptibility passes through a maximum at the latter temperature (Fig. 29). Although the susceptibility decreases with increase of the field intensity, the magnetization hysteresis is absent at all temperatures down to 1.3°K, which, in the opinion of Bozorth and Van Vleck,<sup>[86]</sup> indicates the absence of ferromagnetic ordering in europium. An electrical resistance maximum, characteristic of a transition to the antiferromagnetic state, is also found at the Néel temperature at 90°K.<sup>[87]</sup> Measurements of various physical properties indicate that the europium ion in the metal is divalent between the melting point and 5°K. Bozorth and Van Vleck<sup>[86]</sup> point out, however, that the observed high value of the magnetic susceptibility of europium and its increase below 50°K, cannot be explained by assuming that europium is in

FIG. 29. Temperature dependence of the molar magnetization of europium.



the divalent state, but that it is necessary to assume that at low temperatures the europium ion is in the trivalent state. The reason for this contradiction is not yet clear. Henry<sup>[20]</sup> measured the magnetization of europium in fields up to 100,000 Oe and found that at 4.2°K the magnetization is a complex function of the field. From this, Henry concluded that there are two different exchange interactions in europium. This conclusion was confirmed by recent neutron-diffraction studies,<sup>[88]</sup> which indicated a helicoidal magnetic structure or an amplitude modulation of the magnetic moment with a period of 3.6 a<sub>0</sub>.

6. MAGNETOELASTIC PROPERTIES OF RARE-EARTH FERROMAGNETS

We have already reported that one of the causes of the complex magnetic behavior of r.e.f.'s may be the strong dependence of the exchange interaction between basal layers on the interatomic distance. In this connection, a study of the various magnetoelastic effects in r.e.f.'s is of great interest, because it should give useful information on the nature of the helicoidal magnetic ordering.

1. Magnetostriction in the Ferromagnetic Region.

The magnetostriction of dysprosium has been studied most extensively.<sup>[13,39,90]</sup> Figure 30 shows the isotherms of λ<sub>||</sub> and λ<sub>⊥</sub> for Dy both at T < θ<sub>1</sub> and at T > θ<sub>1</sub> (θ<sub>1</sub> = 85°K). It is evident that the magnetostriction is unusually strong: λ<sub>||</sub> is of the order of 10<sup>-3</sup> in fields of 15,000 Oe, which are still far from saturation. Although this magnetostriction was measured in polycrystalline samples, we can state with assurance that it is due to the processes of the rotation of the magnetic moments of the layers in the basal plane against the opposition of the magnetic anisotropy forces. This follows from the following considerations: first, the anisotropy along the hexagonal axis is so strong that in fields of 10–20 kOe the magnetic moments remain in the basal plane. Second, the strong magnetostric-

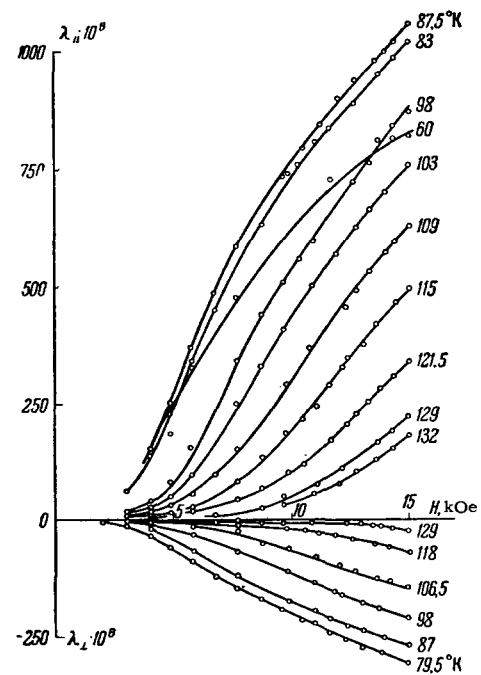


FIG. 30. Isotherms of the longitudinal λ<sub>||</sub> and transverse λ<sub>⊥</sub> magnetostriction of dysprosium near the temperature θ<sub>1</sub>.

tion of Fig. 30 is observed both in the ferromagnetic state (below θ<sub>1</sub>), as well as above this temperature, in fields stronger than H<sub>CR</sub> (in such fields, the helicoidal structure is absent and the metal behaves like a ferromagnet). In this range of fields, the magnetic moments in the basal plane are rotated by the field which overcomes the magnetic anisotropy forces. Figure 30 shows that λ<sub>||</sub> and λ<sub>⊥</sub> have different signs. This means that the magnetostriction in the basal plane is anisotropic. When the temperature is increased, the striction due to the magnetic anisotropy forces in the basal plane decreases monotonically together with that magnetic anisotropy. Since the magnetic anisotropy in

polycrystalline r.e.f. is enormous, it is difficult to reach magnetic saturation and, therefore, we did not obtain maximum values of the magnetostriction. Recent measurements of the magnetostriction in single crystals of Dy and Ho<sup>[91]</sup> gave values of  $\lambda_{||}$  reaching  $5000 \times 10^{-6}$ .

A study of the magnetostriction of terbium<sup>[92,93]</sup> showed that in the ferromagnetic region, at  $T < \theta_1 = 219^\circ\text{K}$ , its striction is also anisotropic and very high ( $\lambda_{||} = 750 \times 10^{-6}$  at  $85^\circ\text{K}$  and  $H = 15$  kOe); this striction is also due to the processes of the rotation of the magnetic moments against the opposition of the magnetic anisotropy forces.

The magnetostriction of erbium in the ferromagnetic region could be measured only in fields up to 5 kOe at  $T = 4.2^\circ\text{K}$  ( $\theta_1$  lies below  $20^\circ\text{K}$ ). The magnetostriction was also of the order of  $10^{-3}$ .\*

The magnetostriction of polycrystalline Gd was measured in the work reported in<sup>[13,9]</sup>. The magnetostriction of this metal behaves in a complex way and has not yet been interpreted. It changes its sign at  $220^\circ\text{K}$  in fields of 1000–2000 Oe. Recent measurements of the magnetostriction, carried out on a single crystal of Gd,<sup>[96]</sup> are still insufficient for the understanding of the singularities in the magnetostriction of polycrystalline Gd.

As already reported (p. 189), the anisotropic magnetostriction gives rise to a considerable effective magnetoelastic energy field and affects markedly the position of the point  $\theta_1$ . The effective field of the magnetoelastic energy should have a particularly strong influence on the point  $\theta_1$  of terbium, because in this r.e.f. the critical field  $H_{\text{CR}}$  is an order of magnitude smaller than in dysprosium, holmium, and erbium.

**2. "Helicoidal" Magnetostriction.** The second interesting feature of the magnetostrictive properties of r.e.f. is the presence of a striction effect due to the destruction of the helicoidal magnetic structure.

When the helicoidal magnetic structure is destroyed in fields  $H > H_{\text{CR}}$ , the angle between the magnetic moments lying in different hexagonal layers varies from several tens of degrees to zero. This should be accompanied by a considerable change of the exchange interaction energy and, consequently, by a change of the spontaneous magnetostriction due to the interaction between layers. This effect was observed in Dy.<sup>[95]</sup> Figure 31 shows the isotherms of  $\lambda_{||}$  and  $\lambda_{\perp}$  in the temperature range  $\theta_2 - \theta_1$ . It is seen that these isotherms are complex.

In fields lower than  $H_{\text{CR}}$ , the longitudinal striction  $\lambda_{||}$  is positive, while the transverse quantity  $\lambda_{\perp}$  is negative. When the field rises to the critical value, the helicoidal structure is destroyed and the energy of the exchange interaction between layers changes

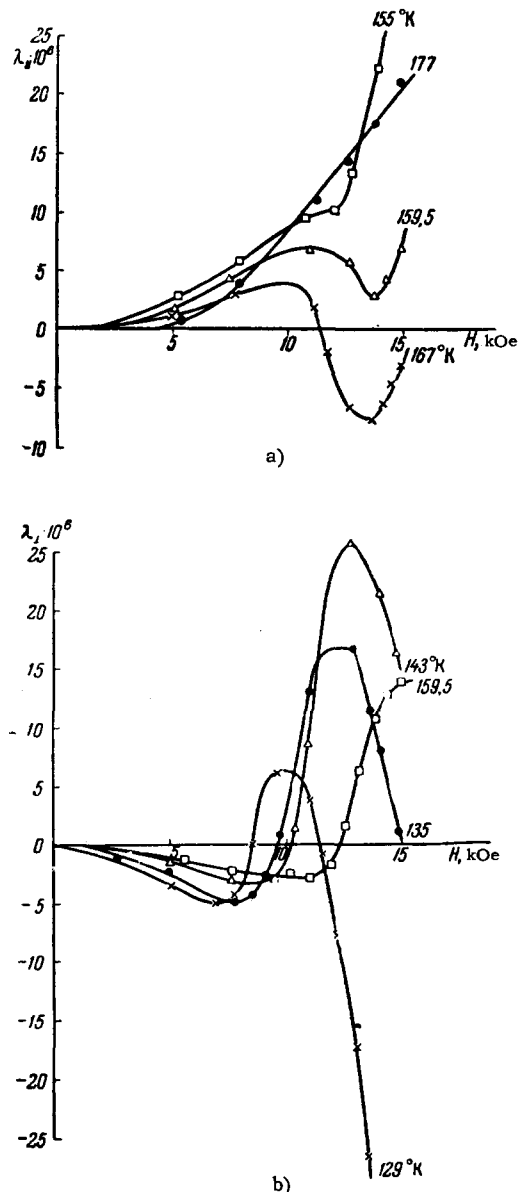


FIG. 31. Isotherms of the magnetostriction of dysprosium between  $\theta_1$  and  $\theta_2$ : a) longitudinal; b) transverse.

sharply, with  $\lambda_{||}$  acquiring a negative component and  $\lambda_{\perp}$  a positive one; consequently, the signs of  $\lambda_{||}$  and  $\lambda_{\perp}$  are reversed. In stronger fields,  $\lambda_{||}$  and  $\lambda_{\perp}$  assume their initial signs. The appearance in the magnetostriction isotherms of components of the opposite sign ( $\lambda_{||} > 0$  and  $\lambda_{\perp} < 0$ ) indicates the presence of the "helicoidal magnetostriction," i.e., the magnetostriction effect due to the change in the exchange interaction between layers on the application of  $H = H_{\text{CR}}$ .

The "helicoidal striction" could not be found in Tb in the range  $\theta_2 - \theta_1$ . This may be explained by the fact that the small value of the critical field of Tb ( $H_{\text{CR}} \approx 100$  Oe) should correspond to a small change of the energy on destruction of the helicoidal structure and therefore the striction effect should be small. In the

\*Measurements were carried out in our laboratory by L. A. Malevskaya and V. I. Sokolov.



case of Ho, Er, and Tm, whose critical fields are high (over 18,000 Oe), strong magnetic fields are necessary to detect the "helical magnetostriction."

We shall calculate the "helical magnetostriction" due to a change of the exchange interaction on transition from the helical antiferromagnetism to ferromagnetism as a function of the magnetic field applied in the basal plane of a hexagonal crystal. We shall neglect the magnetic anisotropy energy (and, therefore, the anisotropic magnetostriction) in the basal plane because in Dy this energy is small at  $T > 110^\circ\text{K}$ .

We assume that the integrals of the exchange interaction between the neighboring layers,  $I_1$ , and between the alternate layers,  $I_2$ , in hexagonal lattices of r.e.f. depend in the following way on the elastic deformation:

$$\left. \begin{aligned} I_1 &= I_{10} + e_1 u_{zz}, \\ I_2 &= I_{20} + e_2 u_{zz}, \end{aligned} \right\} \quad (18)$$

where  $u_{zz}$  is the relative deformation along the  $z$ -axis, directed along the hexagonal  $c$ -axis;  $e_1$  and  $e_2$  are the magnetoelastic (exchange) coupling constants; and  $I_{10}$ ,  $I_{20}$  are constants. Using the expression for the elastic energy of a hexagonal crystal taken from [97], we obtain for the exchange interaction integrals

$$\left. \begin{aligned} I_1 &= I_{10} + e_1 [S_{33} T_{zz} + S_{13} (T_{xx} + T_{yy})], \\ I_2 &= I_{20} + e_2 [S_{33} T_{zz} + S_{13} (T_{xx} + T_{yy})], \end{aligned} \right\} \quad (18')$$

where  $T_{ij}$  are the components of the elastic stress tensor; and  $S_{ij}$  are the elastic compliance constants. Using the expression for the thermodynamic potential  $\Phi$  that includes the elastic energy of a helical magnetic substance in  $H \neq 0$  [cf. Eqs. (11) and (15)], and allowing for the dependence of the exchange interaction integrals on stress, as given by Eq. (18), we can find the helical magnetostriction from the relationship  $u_{ij} = -(\partial\Phi/\partial T_{ij})_{T_{ij}=0}$ .

The calculations lead to the following expressions for  $u_{zz}$  in various magnetic fields:

1) for  $0 < H < H_{\text{Cr}}$

$$u_{zz} = N\mu_S^2 S_{33} (e_1 \cos \alpha_0 + e_2 \cos 2\alpha_0) + \frac{N}{2} \chi_0 D S_{33} H^2; \quad (19)$$

2) for  $H_{\text{Cr}} < H < H_0 = 2.06 H_{\text{Cr}}$

$$u_{zz} = N\mu_S^2 (e_1 + e_2) S_{33} + N\mu S_{33} [(L - K)H^2 - 2LH_0H + (K + L)H_0^2]; \quad (20)$$

3) for  $H \geq H_0$

$$u_{zz} = N\mu_S^2 S_{33} (e_1 + e_2). \quad (21)$$

Here,  $N$  is the number of atoms in  $1 \text{ cm}^3$ ;  $\alpha_0$  is the angle between the magnetic moments of the layers when the external stresses are zero;  $\mu_S$  is the magnetization of a layer calculated per atom;  $S_{33}$  is an elastic compliance constant; and  $\chi_0$  is the magnetic susceptibility of a helical magnetic substance in a field  $H < H_{\text{Cr}}$ . The coefficients  $D$ ,  $K$ , and  $L$  are given by the formulas

$$\left. \begin{aligned} D &= \frac{2 \cos^2 \alpha_0 (1 + 4 \cos \alpha_0)}{1 + \cos \alpha_0 - 2 \cos^3 \alpha_0} \left( \frac{e_1}{I_{10}} - \frac{e_2}{I_{20}} \right) - \frac{e_2}{I_{20}}, \\ K &= \frac{1}{[2 + (1 + 2 \cos \alpha_0)^2] H_0} \left[ \frac{e_2}{I_{20}} - \frac{2 \cos \alpha_0}{1 - \cos \alpha_0} \left( \frac{e_1}{I_{10}} - \frac{e_2}{I_{20}} \right) \right], \\ L &= -\frac{4 \cos \alpha_0 (1 + 2 \cos \alpha_0)}{[2 + (1 + 2 \cos \alpha_0)^2] H_0} \left( \frac{e_1}{I_{10}} - \frac{e_2}{I_{20}} \right). \end{aligned} \right\} \quad (22)$$

The magnetostriction in the basal plane,  $u_{xx}$  and  $u_{yy}$ , is found from (19)–(21) by replacing  $S_{33}$  with another elastic compliance constant  $S_{13}$ . It should be noted that the "helical magnetostriction" between layers is anisotropic and, in general, may have different signs in the basal plane ( $u_{xx}$  and  $u_{yy}$ ) and along the hexagonal axis ( $u_{zz}$ ), because both  $u_{xx}$  and  $u_{yy}$  are proportional to the constant  $S_{13}$  and  $u_{zz}$  is proportional to the constant  $S_{33}$ , which is not equal to  $S_{13}$  and may have a different sign. This explains the fact that  $\lambda_{\parallel}$  and  $\lambda_{\perp}$  of the "helical magnetostriction" of polycrystalline dysprosium have opposite signs (cf. Fig. 31). It follows from Eqs. (2)–(4) that the "helical magnetostriction" in the region  $0 < H < H_{\text{Cr}}$  is proportional to the square of the field, while in the region  $H_{\text{Cr}} < H < H_0$  it varies parabolically, reaching saturation at  $H = H_0 = 2.06 H_{\text{Cr}}$  (Fig. 32, a–c). The magnitude and sign of the magnetostriction is in each region governed by the quantities  $I_{10}$ ,  $I_{20}$ ,  $I_1$ ,  $I_2$ ,  $S_{13}$ ,  $S_{33}$ , and  $\alpha_0$ . For some ranges of the values of these parameters, the striction depends in a complex way on the field, changing sign in the critical field  $H_{\text{Cr}}$  (cf. Fig. 32). Such a dependence of the "helical magnetostriction" on the field explains qualitatively the complex nature of the isotherms  $\lambda(H)$  of dysprosium (cf. Fig. 31).

**3. Intrinsic Magnetostriction.** The third feature of the magnetostriction properties of r.e.f. is the anisotropy of the intrinsic magnetostriction.

As is known, the intrinsic magnetostriction is isotropic ( $\lambda_{\parallel} = \lambda_{\perp}$ ) in cubic ferromagnets because it corresponds to an isotropic exchange interaction. This

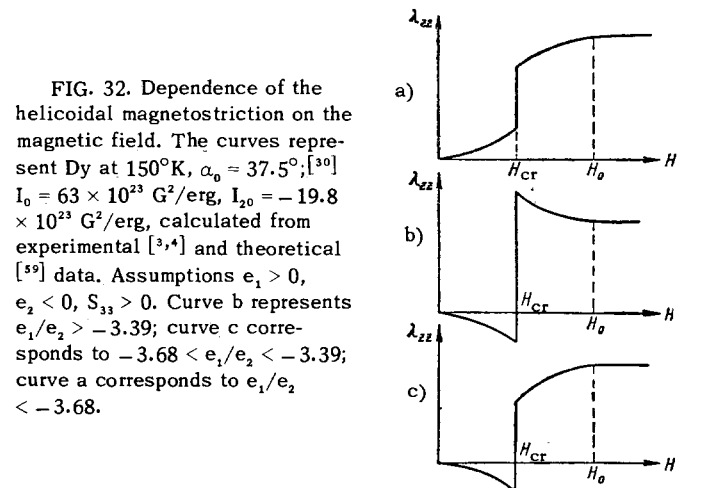


FIG. 32. Dependence of the helical magnetostriction on the magnetic field. The curves represent Dy at  $150^\circ\text{K}$ ,  $\alpha_0 = 37.5^\circ$ ; [30]  $I_0 = 63 \times 10^{23} \text{ G}^2/\text{erg}$ ,  $I_{20} = -19.8 \times 10^{23} \text{ G}^2/\text{erg}$ , calculated from experimental [3,4] and theoretical [59] data. Assumptions  $e_1 > 0$ ,  $e_2 < 0$ ,  $S_{33} > 0$ . Curve b represents  $e_1/e_2 > -3.39$ ; curve c corresponds to  $-3.68 < e_1/e_2 < -3.39$ ; curve a corresponds to  $e_1/e_2 < -3.68$ .

intrinsic magnetostriction isotropy appears clearly near the Curie point. Measurements<sup>[93,95]</sup> showed that the intrinsic magnetostriction  $\lambda_{||}$  of Dy and Tb near  $\theta_2$  is much larger than  $\lambda_{\perp}$  although the two quantities are of the same positive sign: in the case of Tb,  $\lambda_{||}$  near  $\theta_2$  is two orders of magnitude greater than  $\lambda_{\perp}$  (Fig. 33). Thus, the intrinsic magnetostriction of r.e.f. is "anisotropic." This was confirmed recently by the measurements of Bozorth and Wakiyama,<sup>[96]</sup> carried out on a single crystal of Gd. It was found that near  $\theta_2$  the magnetostriction along the c-axis is approximately 20 times higher than that along the a-direction in the basal plane. Such anisotropy of the intrinsic magnetostriction of r.e.f. is due to the different nature of the dependence of the interaction on the interatomic spacings along the axes c and a.

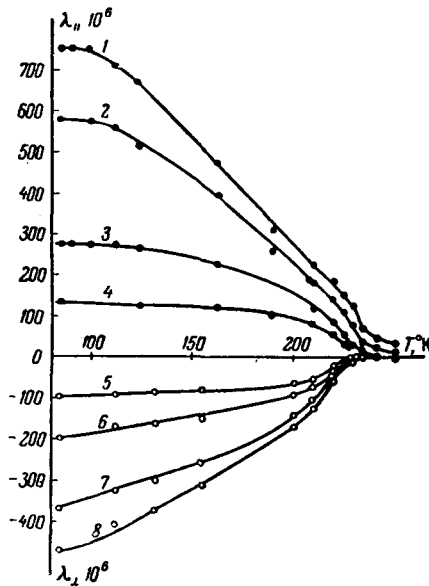


FIG. 33. Temperature dependence of the longitudinal (black dots) and transverse (open circles) magnetostriction of terbium.

This is supported by measurements of the thermal expansion of r.e.f. X-ray diffraction studies showed that large (negative) ferromagnetic anomalies of the lattice parameter occur also below  $\theta_2$  along the c-axis, while they are small along the a-axis.<sup>[64]</sup> Discontinuities in the lattice parameters of dysprosium were observed on passing through the point  $\theta_1$ ;<sup>[98]</sup> this is related to the influence of the anisotropic magnetostriction.

**4. Magnetic Anomalies of the Elastic Moduli.** The difference in the nature of the exchange interactions along the c-axis and in the basal plane is supported also by the measurements of the temperature dependence of the elastic moduli of r.e.f. carried out on polycrystalline samples.<sup>[13,92,99]</sup>

Figure 34 shows the curves of the temperature dependence of the elastic moduli of dysprosium and gad-

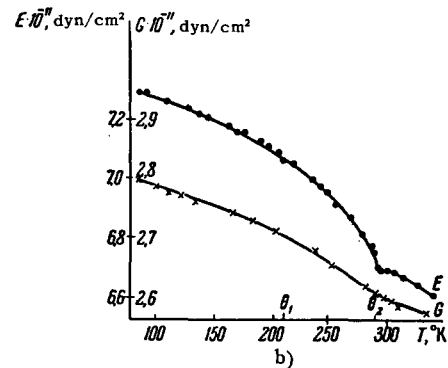
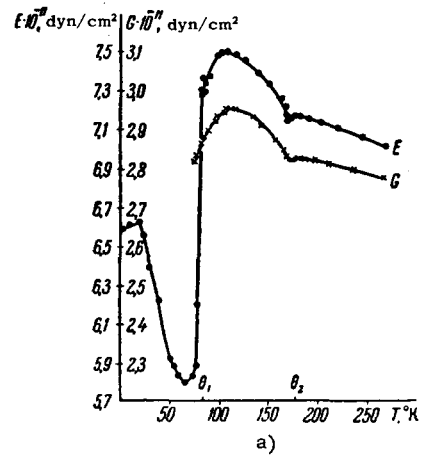


FIG. 34. Temperature dependence of Young's modulus (E) and bulk modulus (G) for dysprosium (a) and gadolinium (b).

olinium. It is seen that the shear modulus G of dysprosium in the region of  $\theta_2$  exhibits the same anomaly as Young's modulus E. As is known, no shear modulus anomalies occur in cubic ferromagnets of the iron group at the Curie point, because shear deformation does not change the volume and, therefore, the energy of the exchange interaction is unaffected in view of the isotropy of the exchange interaction in the crystal lattice. In r.e.f., owing to the anisotropy of the exchange interaction, the change in shape of a crystal in the case of shear deformation should alter the exchange interaction in the lattice, which in its turn should give rise to a shear modulus anomaly in the region of  $\theta_2$ .

Figure 34 shows also that the elastic moduli of Dy decrease sharply on approaching  $\theta_1$ . A similar temperature dependence of the elastic moduli is exhibited by Er and Ho. The reduction of the elastic moduli on approaching the temperature  $\theta_1$  can be explained as follows. Above the point  $\theta_1$ , the elastic stresses deform the helicoid, doing work to overcome the magnetic anisotropy forces in the basal plane as well as the exchange interaction forces between planes. Below  $\theta_1$  (in the ferromagnetic state), the magnetic moments in neighboring basal planes remain parallel under the action of elastic stresses and work is done

only in overcoming the magnetic anisotropy forces in the basal plane. Therefore, the Young's modulus anomalies in the ferromagnetic region are greater than in the helicoidal state, although the values of the magnetostriction and anisotropy constants are approximately the same 10–15 deg below and above the point  $\theta_1$ .

5. Displacement of the Ferromagnetic-Antiferromagnetic Transition Point under Uniform Pressure. The strong sensitivity of the exchange interaction (between layers) to changes of the interatomic spacings along the c-axis in r.e.f. lattices is indicated also by experiments on the influence of pressure on the transition point  $\theta_1$  of Dy.<sup>[100]</sup>

Figure 35 shows the curves  $\sigma(T)$  for Dy recorded in a magnetic field of 3100 Oe under a pressure of 1800 atm and without pressure. Under the action of a uniform pressure, the steep part of the  $\sigma(T)$  curve is displaced parallel to itself, by approximately 7 deg, toward lower temperatures. This means that the point  $\theta_1$  is displaced toward lower temperatures by the same amount. The maximum of the  $H_c(T)$  curve, which is observed in polycrystalline Dy near  $\theta_1$ , is also displaced in the same direction by the same amount.

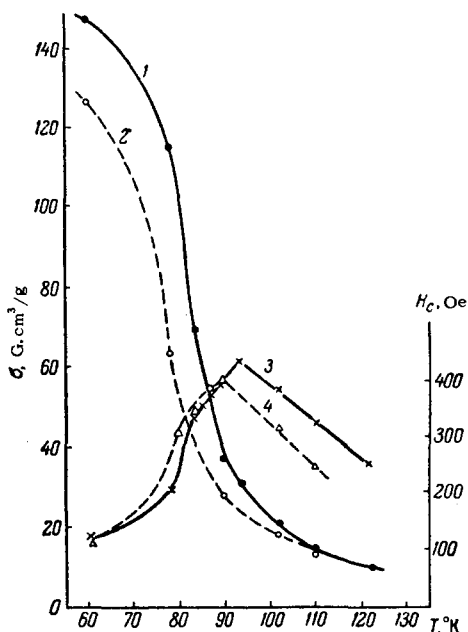


FIG. 35. Displacement of the transition point  $\theta_1$  of dysprosium under pressure. 1) Temperature dependence of the magnetization at 1 atm; 2) temperature dependence of the magnetization at 1800 atm; 3) coercive force at 1 atm; 4) coercive force at 1800 atm.

We mentioned earlier that it follows from thermodynamic considerations that the magnetic anisotropy and magnetoelastic energies in the basal plane, which increase on cooling and the approach to  $\theta_1$ , reduce the critical field  $H_{cr}$  [cf. Eq. (16)].

On the other hand,  $\theta_1$  is related to  $H_{cr}$ ; experiments show that in dysprosium

$$H_{cr} = h(T - \theta_1), \quad (23)$$

where  $h$  is a numerical coefficient. Differentiating this expression with respect to pressure, we find

$$\frac{\partial \theta_1}{\partial P} = -\frac{1}{h} \frac{\partial H_{cr}}{\partial P}. \quad (24)$$

From Eqs. (16) and (24), we obtain

$$\frac{\partial \theta_1}{\partial P} = -\frac{1}{h} \frac{\partial H_{cr}^0}{\partial P} + \frac{1}{h} \frac{\partial}{\partial P} \left( \frac{K}{M_s} + \frac{\lambda^2 E}{M_s} \right). \quad (25)$$

From the above formula, it is evident that the shift of  $\theta_1$  under the action of pressure may, in general, be the result of a change of the exchange interaction between layers [the first term in Eq. (25)], and of a change of the total magnetic anisotropy and magnetoelastic energy [the second term in Eq. (25)].

Experiments showed<sup>[100]</sup> that in the ferromagnetic region at 60°K a uniform pressure reduced the magnetization of Dy in the technical magnetization region. It follows that we can expect only an increase of the effective field of the anisotropy and magnetoelastic energies under the action of pressure.

This increase should, according to Eq. (25), displace  $\theta_1$  toward higher temperatures, whereas in fact the observed displacement is toward lower temperatures, in agreement with the minus sign of the first term in Eq. (25). This can be explained by the stronger rise of the effective field of the exchange interaction between layers, on the application of pressure, due to the strong dependence of this interaction on the distance between layers.

The method just described was used also to carry out tests on the influence of a uniform pressure on the point  $\theta_1 = 210^\circ\text{K}$  of polycrystalline gadolinium. At this point, a sharp drop of the weak-field magnetization and a minimum of the coercive force are observed. Figure 36 gives the curves of the temperature dependence of

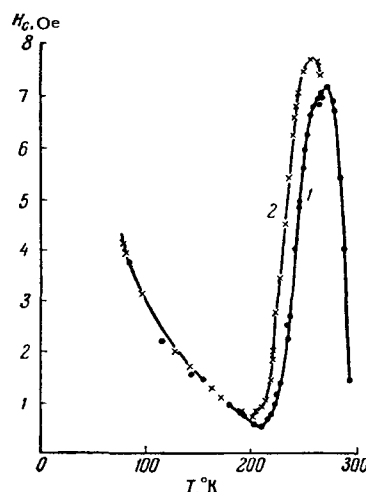


FIG. 36. Displacement of the point  $\theta_1$  of gadolinium under pressure. 1) Temperature dependence of the coercive force at 1 atm; 2) temperature dependence of the coercive force at 1800 atm.

$H_C$  at pressures of 1 and 1800 atm. It is seen that the minimum of  $H_C$  is displaced toward lower temperatures by about 10 deg. This displacement is obviously also due to a change in the exchange interaction between the basal planes of the hexagonal lattice of gadolinium under the influence of uniform pressure. A more detailed interpretation of the results of these tests will be possible after one has obtained data on the nature of the magnetic structure of this metal.

In interpreting the experiments on the influence of the interatomic spacings on the magnetic structure of r.e.f. we should, in general, allow for the change in the exchange integral due to the deformation of the Fermi surface. However, a theoretical analysis carried out for Gd<sup>[101]</sup> shows that the influence of this factor is very small and can be neglected.

Theoretical work<sup>[47,48,49]</sup> has shown that the exchange interaction in r.e.f. is of an indirect nature (exchange via conduction electrons or via electrons of the closed 5s<sup>2</sup>- and 5p<sup>6</sup>-shells). In view of the long-range nature of this interaction, it would seem that it should give a smoother dependence of the exchange interaction on the interatomic spacings than is the case for the direct exchange, which occurs, for example, in Ni and Fe. This does not agree with the results of the measurements of the magnetoelastic effects in r.e.f., which indicate a strong dependence of the indirect exchange on the interatomic spacings (along the c-axis). Another incomprehensible fact is that the indirect exchange in the basal plane is practically insensitive to changes in the interatomic spacings; a theoretical explanation of these problems would help in understanding further the magnetic nature of r.e.f.

## 7. ELECTRICAL AND GALVANOMAGNETIC PROPERTIES OF RARE-EARTH FERROMAGNETS

Electrons of the 4f-shells in rare-earth atoms are screened by the 5s- and 5p-shell electrons and, apparently (in contrast to the 3d-electrons of metals of the iron group), do not go over into the collective state

and do not take part in conduction. However, due to the exchange coupling between the "magnetic" 4f-electrons and the conduction electrons, r.e.f. exhibit strong anomalies in the temperature dependence of the electrical resistance.

Figures 37 and 38 show the temperature dependences of the resistivity of single crystals of dysprosium<sup>[103]</sup> and erbium.<sup>[7]</sup> The temperature dependences of the resistance of other r.e.f. are of a similar nature.<sup>[11,22,102,104-106]</sup> The following point is worth noting. Compared with normal metals and even transition metals of the iron group, r.e.f. have very high electrical resistivity (at room temperature, the resistivity  $\rho$  is of the order of  $100 \times 10^{-6} \Omega\text{-cm}$ ). Below the transition temperature  $\theta_2$ , the temperature coefficient of the resistance increases very rapidly.

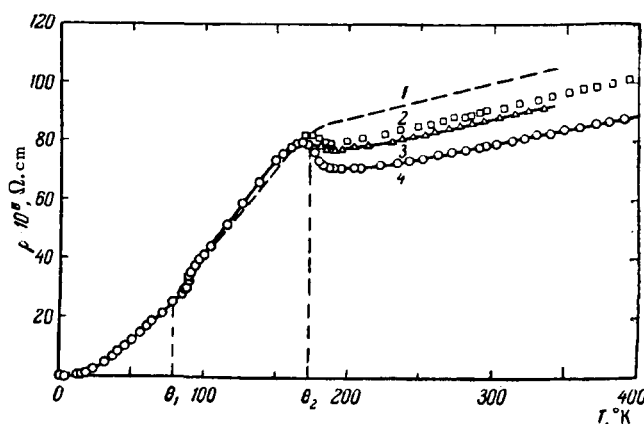


FIG. 37. Temperature dependence of the electrical resistivity of a dysprosium single crystal. 1) Single crystal, in the basal plane; 2) polycrystalline sample; 3) single crystal, in a direction making 42° with the hexagonal axis; 4) single crystal, in a direction making 18° with the hexagonal axis.

In the region of the paramagnetic-antiferromagnetic transition itself, several r.e.f., including Gd (which is another proof of the existence of antiferromagnetic ordering in this metal), exhibit a change of the nature of their conduction: metallic conduction is replaced

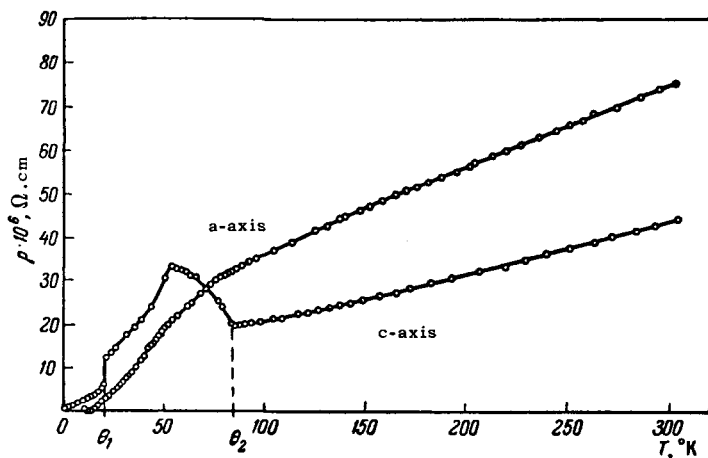


FIG. 38. Temperature dependence of the electrical resistance of an erbium single crystal.

by semiconducting behavior. At the point of transition from the antiferromagnetic to the ferromagnetic state,  $\theta_1$ , there is also a resistance anomaly (cf. Figs. 37 and 38) but this is much smaller than the anomaly at the point  $\theta_2$ , and is not observed in all r.e.f. It is worth noting also that the resistance anomalies are strongly anisotropic: anomalies at the points  $\theta_1$  and  $\theta_2$  are much larger along the  $c$ -axis of the crystal than in the basal plane.

It is known that the resistivity of normal metals consists of the residual resistivity,  $\rho_{\text{res}}$ , due to the scattering of electrons on impurities and crystal structure defects, and of the resistivity,  $\rho_{\text{phon}}$ , due to the scattering of electrons on the lattice vibrations (phonons). In the ferromagnetic and antiferromagnetic metals, there is one more electron scattering mechanism: the scattering on magnetic inhomogeneities (magnons), which is responsible for the magnetic anomaly of the resistivity  $\rho_{\text{mag}}$ . For brevity, we shall call  $\rho_{\text{mag}}$  the magnetic resistivity. Thus the resistivity of ferro- and antiferromagnets consists of the following components:

$$\rho = \rho_{\text{res}} + \rho_{\text{phon}} + \rho_{\text{mag}}. \quad (26)$$

Following Kasya<sup>[107]</sup> and de Gennes<sup>[108]</sup>, the magnetic component of the resistance of r.e.f. can be described by allowing for the exchange interaction between the localized 4f-electrons and the conduction electrons. It is assumed that this interaction depends on the relative orientation of the spin of the  $s$ -conduction electrons and the resultant spin of the 4f-shell. At 0°K, all the 4f-spins are ordered and the  $f$ - $s$  exchange interaction has the same periodicity as the crystal field: consequently, the magnetic resistance is equal to zero. When the temperature is increased, the magnetic order is disturbed and, therefore, the  $f$ - $s$  interaction ceases to be strictly periodic. This gives rise to the additional "magnetic" resistance which increases on approach to the magnetic transition point  $\theta_2$ . Above this point, at temperatures such that the ordering of the 4f-shell spins is completely destroyed and the periodicity of the  $f$ - $s$  interaction disappears, the magnetic resistance becomes greatest and independent of temperature. Kasya<sup>[107]</sup> showed that the additional magnetic resistance of r.e.f. depends on the spin  $S$  of the 4f-shell and on the average value of the resultant spin  $\bar{\sigma}$  of the ion (which is proportional to the magnetization) at a given temperature:

$$\rho_{\text{mag}} = c(S - \bar{\sigma})(S + \bar{\sigma} + 1), \quad (27)$$

where the constant  $c$  is proportional to the  $f$ - $s$  exchange-interaction integral. Above the point  $\theta_2$ , the average spin is  $\bar{\sigma} = 0$  and

$$(\rho_{\text{mag}})_{T > \theta_2} = cS(S + 1). \quad (28)$$

Subtracting Eq. (28) from Eq. (27), we find that the anomalous reduction of the electrical resistance of r.e.f. below the point  $\theta_2$  is equal to

$$\Delta \rho_{\text{mag}} = c\bar{\sigma}(\bar{\sigma} + 1). \quad (29)$$

Since, at  $T = 0^\circ\text{K}$ , the spins are completely ordered,  $\bar{\sigma} = S$  and

$$(\Delta \rho_{\text{mag}})_{T=0^\circ\text{K}} = (\rho_{\text{mag}})_{T > \theta_2} = cS(S + 1). \quad (30)$$

The latter formula was checked for r.e.f. in <sup>[102]</sup>. It follows from Fig. 39 that there is quite good agreement with the experimental data: the magnetic resistance of various r.e.f. at 0°K is proportional to  $S(S + 1)$ .

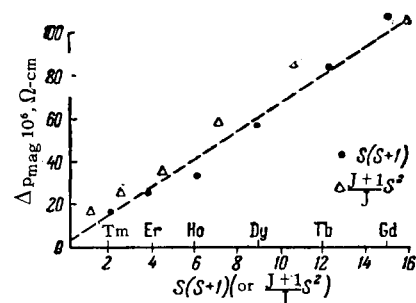


FIG. 39. Dependence of the magnetic resistivity of rare-earth ferromagnets at  $T > \theta_2$  on the 4f-shell spin  $S$  and on the total angular momentum  $J$ .

In the calculations quoted above, an allowance was not made for the influence of the orbital angular momentum of the 4f-shell. Later, <sup>[109]</sup> it was shown that if the orbital angular momentum is allowed for the magnetic resistance is equal to (when  $T > \theta_2$ )

$$(\rho_{\text{mag}})_{T > \theta_2} = c \frac{J+1}{J} S^2, \quad (31)$$

where  $J$  is the total angular momentum of the 4f-shell. This result, however, does not differ greatly from the preceding one because the factor  $(J + 1)/J$  does not vary greatly from one r.e.f. to another. Therefore, the experimental results are described by Eq. (30) as satisfactorily as by Eq. (31). Recently, a study was made of the resistance of several rare-earth alloys.<sup>[151]</sup> It was found that the magnetic resistance of these alloys also obeys Eq. (31).

The theory given above does not explain the phenomenon of the transition from metallic to semiconducting behavior, observed in the region of  $\theta_2$  in several r.e.f. An explanation of this phenomenon was given in the work of Turov and Irkhin.<sup>[110,111]</sup> They showed that on the transition of a metal from the paramagnetic to the antiferromagnetic state the energy spectrum of the conduction electrons alters and an energy gap appears. Since the magnetization near the point  $\theta_2$  depends strongly on temperature, it is precisely in this region of temperatures that the largest deviations from the metallic conduction should be observed, and, in particular, that the transition to semiconducting behavior is possible. For helicoidal antiferromagnets, this problem was discussed in the work of Miwa<sup>[112]</sup> and Macintosh.<sup>[113]</sup> They showed that in the case of a helicoidal magnetic structure there is an additional resist-

ance (compared with the fully disordered state). This additional "helical" magnetic resistance appears because the helical period is not, in general, a multiple of the crystal lattice period. For this reason, the periodicity of the Coulomb interaction field between the 4f-electrons and the conduction electrons differs from the periodicity of the crystal lattice. This causes additional "helical" scattering of electrons, which is absent in the ferromagnetic and paramagnetic states. On transition from the helical to the ferromagnetic structure at the point  $\theta_1$ , the "helical" scattering of the conduction electrons disappears and this leads to a reduction of the electrical resistance, a fact that has been observed experimentally for several r.e.f. However, a reduction of the electrical resistance at the point  $\theta_1$  is observed only in metals for which the energy change on transition from the helical to the ferromagnetic state is relatively large. In the case of other substances (for example, terbium), whose energy changes slightly on transition at the point  $\theta_1$ , the resistance anomalies at this point are not noticeable. It is interesting to note that the destruction of the helical magnetic structure by the field destroys the resistance jump at  $\theta_1$ .<sup>[103]</sup>

The anisotropy of the electrical resistance anomalies of single crystals of dysprosium, erbium, and holmium (Figs. 37 and 38) is explained by the layered magnetic structure of these metals, as a consequence of which the conditions for the scattering of electrons are different along the hexagonal axis and in the basal plane.

Recently, the thermoelectric power of several r.e.f. was measured.<sup>[114]</sup> It was found that this power has anomalies in the region of the temperatures  $\theta_1$  and  $\theta_2$  (Fig. 40), which also indicates that the conditions for the scattering of electrons change at the magnetic transitions in these substances.

As pointed out earlier, an increase of the long-range magnetic order reduces the resistivity  $\rho_{\text{mag}}$ . A systematic study of the influence of the magnetic order on the resistance of dysprosium, holmium and erbium, under the action of a magnetic field, was reported in [22]; the corresponding work on gadolinium was presented in [115].

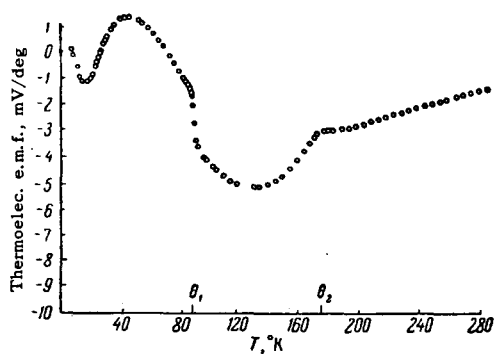


FIG. 40. Temperature dependence of the thermoelectric power of dysprosium.

The field should affect particularly strongly the magnetic resistance near the points  $\theta_1$  and  $\theta_2$ , i.e., where the degree of magnetic ordering increases sharply on application of the field.

Figure 41 gives the temperature dependence of the longitudinal galvanomagnetic effect (magnetoresistance) in dysprosium. It is seen that near the transitions  $\theta_2$  and  $\theta_1$  the negative magnetoresistance reaches its maximum. The magnetoresistance of terbium and holmium is similar. Experiments showed that the magnetoresistance near  $\theta_2$  is isotropic, and that  $(\Delta R/R)_{\parallel}$  and  $(\Delta R/R)_{\perp}$  have the same signs and similar values. Near  $\theta_2$ , the even magnetoresistance is proportional to the square of the intrinsic magnetization. It is interesting to note that the coefficient of proportionality, relating the change of the resistivity to the square of the intrinsic magnetization at  $\theta_2$ , is the same for dysprosium, holmium and terbium, which have the same helical magnetic structure (Fig. 42).

We have already seen that the transition of dysprosium from the helical to the ferromagnetic state at  $\theta_1$  is accompanied by a sharp decrease of the resistance. At the same point  $\theta_1$ , there is also a maximum of the negative longitudinal and transverse magnetoresistances (Fig. 41), due to the destruction of the helical magnetic structure by the field and the transition of the sample to the ferromagnetic state. The reduction of the electrical resistance during this field-induced transition confirms the suggestion that the

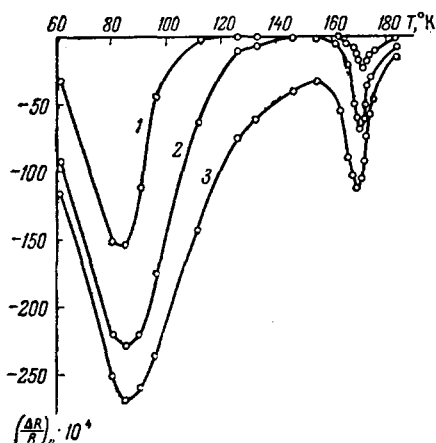
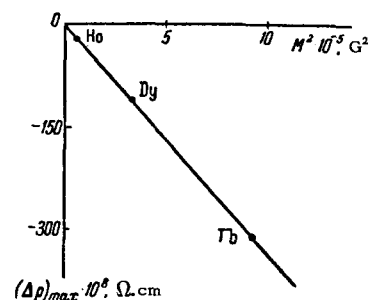


FIG. 41. Temperature dependence of the longitudinal magnetoresistance of dysprosium at: 1) 6500 Oe; 2) 11 500 Oe; 3) 15 000 Oe.

FIG. 42. Dependence of the magnetoresistance of dysprosium, holmium, and terbium on the square of the intrinsic magnetization at the point  $\theta_2$ .



scattering of electrons on the magnetic inhomogeneities in the ferromagnetic state is weaker than in the helioidal state. Figure 43 shows the isotherms of the transverse magnetoresistance of dysprosium. It is seen that the absolute value of  $\Delta R/R$  increases strongly after reaching the critical field.

The temperatures of the magnetic transitions  $\theta_1$  and  $\theta_2$  were close to one another in the case of terbium. Therefore, this metal exhibited one magnetoresistance maximum in the temperature range  $\theta_1$  to  $\theta_2$ , but the curve  $(1/R) (\Delta R/\Delta H) (T)$  showed two maxima corresponding to the points  $\theta_1$  and  $\theta_2$  (Fig. 44).

Figure 45 shows the results of measurements of the longitudinal magnetoresistance of gadolinium.\* It is seen that in this metal, as in Tb, there are two maxima: one of them occurs at the Curie point (290°K), and the other at 240–250°K. The nature of the second maximum is not yet clear.

It is of interest to study the Hall effect in r.e.f. As is known, the normal ferromagnetic metals—iron, nickel, and cobalt—have anomalously high values of the Hall emf, two to three orders of magnitude greater than the effects observed in nonferromagnetic metals. It follows from theoretical work<sup>[118,119]</sup> that the anomalous Hall effect of ferromagnets is due to the spin-orbit interaction, which should be different in metals of the iron group and in r.e.f.

In metals of the iron group, the 3d- and 4s-bands overlap, while in rare-earth metals there is no overlap of the 4f- and 6s-bands, i.e., the electron structure of the latter metals differs strongly from the electron structure of the iron-group metals. From this point of view, a systematic study of the Hall effect in

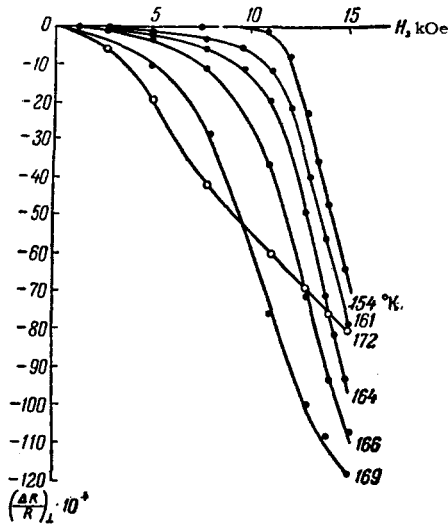


FIG. 43. Isotherms of the transverse magnetoresistance of dysprosium.

\*These measurements were carried out by Yu. V. Ergin in our laboratory.

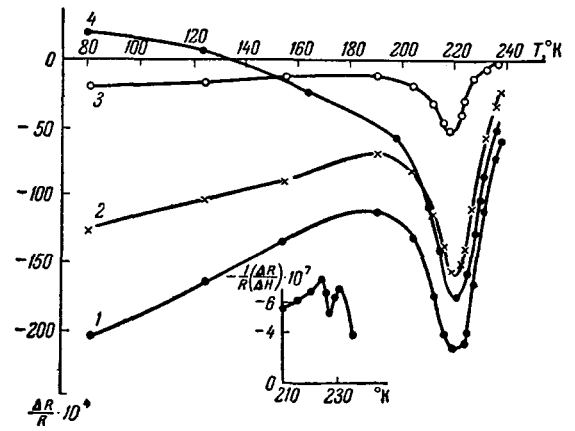


FIG. 44. Temperature dependence of the magnetoresistance of terbium. 1) Longitudinal effect,  $H = 15\,000$  Oe; 2) longitudinal effect,  $H = 7800$  Oe; 3) longitudinal effect,  $H = 1300$  Oe; 4) transverse effect,  $H = 15\,000$  Oe. Lower part of the figure shows the temperature dependence of the slopes of the magnetoresistance isotherms  $(1/R)\Delta R/\Delta H$  in  $H = 14\,000$  Oe.

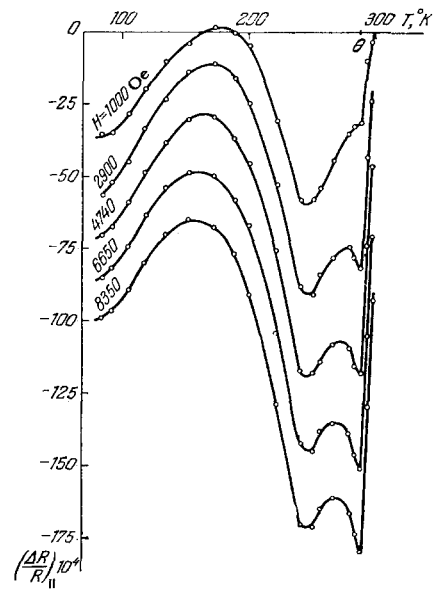


FIG. 45. Temperature dependence of the longitudinal magnetoresistance of gadolinium.

r.e.f. is very important. Particularly interesting are the measurements in the temperature range covering the ferromagnetic-antiferromagnetic and antiferromagnetic-paramagnetic transitions.

The information on the Hall effect in r.e.f. and in other rare-earth metals is very scarce. Several workers<sup>[116,117]</sup> have measured the Hall effect in gadolinium, dysprosium, and erbium, particularly in the paramagnetic region. Above the transition point  $\theta_2$ , the Hall emf was negative and proportional to the magnetic field. On approaching the point  $\theta_2$ , the Hall emf of dysprosium and erbium increased, which was explained by the appearance of the spontaneous Hall effect due to the magnetization.

The numbers of carriers per atom at room temperature (Table II) were determined from the classical Hall coefficient  $R_0$  for all the investigated r.e.f. The same table also lists the numbers of carriers for other rare-earth metals at room temperature.

The Hall effect of Gd in the ferromagnetic region was investigated by Vol'kenshtein and Fedorov.<sup>[120]</sup> They established that the spontaneous Hall coefficient  $R_S$  had a temperature dependence of the same nature as nickel (Fig. 46) except that the gadolinium coefficient was twenty times as large. The maximum on the  $R_S(T)$  curve lay below the Curie point (at about 250°K).

Vol'kenshtein and Fedorov also showed that the spontaneous Hall coefficient was proportional to the magnetic resistance of gadolinium  $\rho_{\text{mag}}$ . The detection of the Hall emf maximum in gadolinium was discussed also in [121].

Table II

Metals	Y	La	Ce	Pr	Nd	Gd	Dy	Er
Number of charge carriers per atom	2.7	2.9	1.6	3	2.11	2.1	1.5	2.1

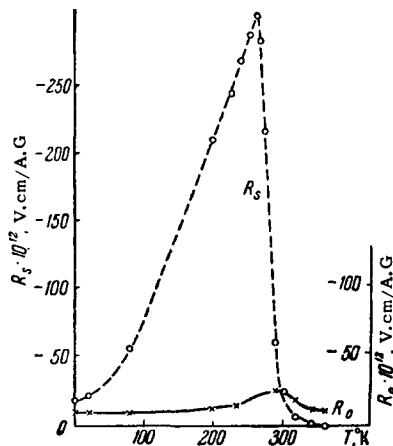


FIG. 46. Temperature dependence of the classical ( $R_0$ ) and spontaneous ( $R_S$ ) Hall coefficients of gadolinium.

Vol'kenshtein and Fedorov also investigated the Hall effect in dysprosium and erbium.<sup>[106]</sup> They found that the Hall emf of dysprosium was negative near the point  $\theta_2$  and positive in the region of the transition  $\theta_1$ . At the transition points themselves, the Hall emf reached extremal values. A maximum of the Hall emf was found in erbium at the point  $\theta_1$ .

Thus, investigations of the electrical and galvanomagnetic properties of r.e.f. lead to the conclusion that there is a strong coupling between the "magnetic"

electrons and conduction electrons. However, in contrast to the d-metals, such an interaction does not lead to any marked participation of the conduction electron spins in the establishment of the magnetic moment. This follows from the fact that for the majority of r.e.f. the magnetic moment per atom differs only by several percent from the theoretically calculated magnetic moment of the corresponding ion.

## 8. MAGNETIC PROPERTIES OF RARE-EARTH ALLOYS

Studies of the magnetic properties of the alloys of rare-earth metals themselves and of rare-earth metals with other metals, both ferromagnetic and nonferromagnetic, are of major interest.\* This is because a change of the atomic neighbors in a rare-earth metal crystal alters the interaction in the crystal, giving another opportunity of studying this interaction in rare-earth ferromagnets and antiferromagnets.

### 1. Intermetallic compounds of rare-earth metals.

The magnetic properties of intermetallic compounds of rare-earth metals and the iron-group metals have been studied in recent years. It was established<sup>[124-127]</sup> that the temperature dependence of the magnetization was anomalous (Fig. 47) in compounds of the  $R\text{Co}_5$  type ( $R = \text{Gd, Tb, Dy, Ho, Er, and Tm}$ ). In some cases, a magnetic compensation point was observed similar to that found in ferrites. On this basis, it has been suggested that in  $R\text{Co}_5$  alloys the Co ions and the rare-earth ions form two magnetic sublattices, the resultant moments of which are oriented antiparallel to each other. Assuming that the atomic magnetic moments of cobalt and the rare-earth element have the same values in the alloy as in the pure metals, we can estimate the effective magnetic moment per molecule of the intermetallic compound  $R\text{Co}_5$ :

$$M_{R\text{Co}_5} = 5M_{\text{Co}} - M_{\text{R}}. \quad (32)$$

Here,  $M_{R\text{Co}_5}$  is the resultant magnetic moment of the

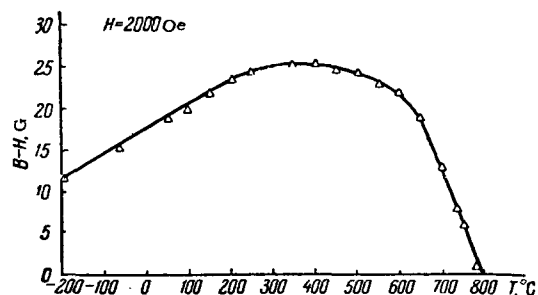


FIG. 47. Temperature dependence of the magnetization ( $B-H$ ) of the intermetallic compound  $\text{Co}_5\text{Gd}$ .

\*A review of the physical properties of rare-earth metal alloys is given in the book by E. M. Savitskii, V. R. Terekhova, I. V. Burov, I. A. Markov, and O. O. Naumkin "Rare-Earth Metal Alloys", Moscow, U.S.S.R. Academy of Sciences Press, 1962.



alloy  $\text{RCo}_5$ ;  $M_{\text{Co}}$  and  $M_{\text{R}}$  are the magnetic moments of the "cobalt" and "rare-earth" sublattices, respectively. If  $R = \text{Ce}, \text{Pr}, \text{Nd}, \text{Sm}, \text{or } \text{Y}$ , then the temperature dependence of the magnetization has the normal "Weiss" form. Figure 48 shows the dependence of the experimental values of the magnetic moments of  $\text{RCo}_5$  alloys on the magnetic moment of the rare-earth metal. The experimental points satisfactorily fit a straight line, with the exception of those for the intermetallic compounds of neodymium and praseodymium, which depart markedly from the straight line. The reason for this departure is not clear, but we may assume that here (as in the case of mixed yttrium-neodymium and yttrium-praseodymium iron garnets<sup>[149]</sup>) the orientation of the orbital magnetic moment of the rare-earth atom exerts a strong influence. This assumption is arrived at as follows. A negative exchange interaction, producing an antiparallel orientation of the spin magnetic moments (Fig. 49), acts between the neodymium (or praseodymium) atoms and the cobalt atoms.

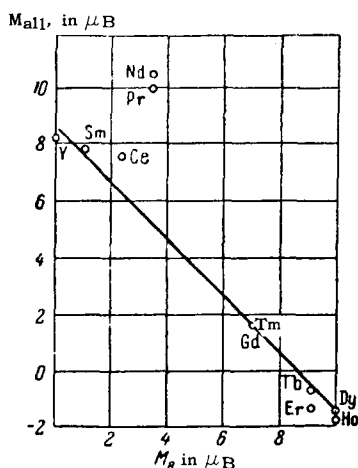


FIG. 48. Dependence of the magnetic moment of  $\text{Co}_5\text{R}$  compounds on the magnetic moment of the rare-earth ion.



FIG. 49. Directions of the spin and orbital momenta in the compounds  $\text{NdCo}_5$  and  $\text{PrCo}_5$ .

Since, for metals of the cerium subgroup  $J = L - S$  (according to Hund's rule), therefore the orbital magnetic moment is directed opposite to the spin moment, but the orbital moment of Nd and Pr has the same direction as the spin moment of Co. This is the reason for the higher magnetic moments of the compounds  $\text{NdCo}_5$  and  $\text{PrCo}_5$  in Fig. 48. However, it is not clear why the points for the compounds of cerium and samarium (for which the rule  $J = L - S$  is also valid) lie very close to the straight line in Fig. 48.

The recent suggestion of the double sublattice structure of  $\text{RCo}_5$  compounds was proved by direct neutron-

diffraction studies.<sup>[128]</sup> It was established that the alloy  $\text{HoCo}_5$  is ferromagnetic and the magnetic moments of cobalt and holmium are directed opposite to each other.

The intermetallic compounds of gadolinium and iron were investigated in<sup>[122,124,129-131]</sup>. In the compounds  $\text{GdFe}_5$ ,  $\text{GdFe}_3$  and  $\text{GdFe}_2$ , there is an antiferromagnetic interaction between the ions of iron and gadolinium, i.e., these compounds also have the sublattice structure. This is confirmed by the observation of a magnetic compensation point in  $\text{GdFe}_5$ .<sup>[131]</sup> However, the magnetic properties of  $\text{GdFe}_5$  cannot be described starting from the assumption of double magnetic sublattice structure. In<sup>[122,130]</sup>, it was shown that  $\text{GdFe}_5$  has three sublattices: two iron, differing by the type of atomic site, and one gadolinium. The value of the magnetic moment per unit cell of  $\text{GdFe}_5$  agrees with the assumption that in one of the iron sublattices the magnetic moments are oriented parallel to the magnetic moment of the gadolinium sublattice, and in the other iron sublattice they are antiparallel to gadolinium.

We note that several intermetallic compounds of rare-earth metals with metals of the iron group have very large values of the coercive force.<sup>[129]</sup> The highest coercive force (8000 Oe) was observed in  $\text{GdCo}_5$ , which was related by the authors of<sup>[129]</sup> to the high anisotropy energy of this alloy. The magnetic properties of the intermetallic compounds of nickel with rare-earth metals were investigated in<sup>[122]</sup>. It was established that compounds of the  $\text{RNi}_5$  type have low Curie points (less than  $40^\circ\text{K}$ ) and behave as normal ferromagnets. A suggestion was made in<sup>[122]</sup> that the magnetic moments of nickel ions in these compounds are disordered. However, the magnetic moments of intermetallic compounds of the  $\text{RNi}_5$  type are somewhat lower than the theoretical values calculated on the assumption that only the rare-earth ions are magnetically ordered.

Cherry and Wallace<sup>[132]</sup> investigated the temperature dependences of the magnetization of intermetallic compounds of the  $\text{RMn}_5$  type, where  $R = \text{Sm}, \text{Gd}, \text{Tb}, \text{Dy}, \text{Ho}, \text{Er}, \text{or } \text{Y}$ , in the temperature range  $80-500^\circ\text{K}$ ; the Curie temperature decreased with increase of the atomic number of the element R: from  $465^\circ\text{K}$ , for a gadolinium compound, to  $415^\circ\text{K}$ , for an erbium compound. In all these compounds, the magnetization rose rapidly on cooling. In the compounds  $\text{DyMn}_5$  and  $\text{TbMn}_5$ , this increase was observed only in sufficiently strong magnetic fields (7000 Oe). In weaker fields (2500 Oe), a maximum was found in the temperature dependence of the magnetization (at  $200^\circ\text{K}$ ). The temperature dependence of the magnetization of the compound  $\text{SmMn}_5$  was similar in shape in weak and strong fields, but even for this alloy an anomaly was found in the temperature dependence of the magnetization at low temperatures. All this indicates that intermetallic compounds of the  $\text{RMn}_5$  type exhibit complex magnetic behavior. It is possible that these compounds also have

magnetic sublattice structure (i.e., they are ferromagnets).

Williams et al.<sup>[133]</sup> reported data on the magnetic properties of intermetallic compounds of the rare-earth metals and aluminum, of the  $RAI_2$  type. The dependence of the magnetic moments of  $RAI_2$  alloys on the atomic number of the rare-earth element is similar to the well-known curve of the magnetic moments of free trivalent ions of rare-earth elements (Fig. 50). The values of the magnetic moments in  $GdAl_2$  differ, however, from those calculated theoretically. Williams et al.<sup>[133]</sup> assumed that the cause of this is the polarization of the conduction electrons by the 4f-electrons. The exchange interaction between the 4f-electrons and the conduction electrons forces the latter to contribute to the magnetic moment. Jaccarino et al.<sup>[134]</sup> came to the same conclusion as a result of measurements of nuclear magnetic resonance in  $RAI_2$  compounds.

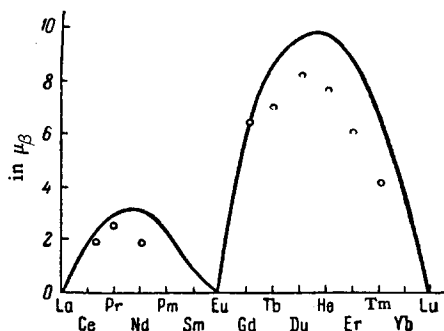


FIG. 50. Magnetic moments of compounds of the  $RAI_2$  type.

It follows from the work of Williams et al.<sup>[133]</sup> that  $RAI_2$  compounds (where  $R = Ce, Pr, Nd, \text{ or } Sm$ ) exhibit ferromagnetism with quite high Curie points. Thus, the Curie point of  $SmAl_2$  is  $122^\circ K$ , and that of  $NdAl_2$  is  $68^\circ K$ . It is known that pure metals of the cerium subgroup are antiferromagnetic (with very low Néel points) or are paramagnetic. However, in the presence of paramagnetic aluminum ions, ferromagnetism is "induced" in  $RAI_2$  compounds. This fact is of great interest. In this connection, we note that Matthias et al.<sup>[135]</sup> established that some alloys of scandium and indium ( $Sc_{1-x}In_x$ ,  $x = 0.238-0.242$ ) are ferromagnetic below  $6^\circ K$ , although pure scandium and indium have paramagnetic properties.

Bozorth et al.<sup>[136]</sup> investigated the magnetic properties of intermetallic compounds of rare-earth metals and metals of the platinum and palladium group:  $RIr_2$ ,  $RRu_2$ , and  $ROs_2$ . The majority of these compounds have ferromagnetic properties. The highest Curie points are those of gadolinium compounds ( $\sim 80^\circ K$ ); the Curie points are lowered when the atomic number of the rare-earth metal is either decreased or increased. The magnetic moment per rare-earth atom in an alloy is found to be smaller than the

moment calculated for trivalent ions and observed in pure rare-earth metals. This is explained by the partial freezing of the orbital magnetic moments by the crystal field of the alloy lattice.

Several workers have investigated the magnetic properties of more complex substances. Williams et al.<sup>[133]</sup> studies the mixed compounds  $Gd_{0.314}Pr_{0.686}Al_2$  and  $Gd_{0.2}Pr_{0.8}Al_2$ . It was found that they have magnetic compensation points at very low temperatures. Williams et al.<sup>[133]</sup> explained this by the influence of the orbital momentum of praseodymium. The spins of gadolinium and praseodymium are parallel to each other but since, for praseodymium,  $J = L - S$ , the resultant magnetic moment of the praseodymium atom is directed opposite to the magnetic moment of the gadolinium atom, which leads to the appearance of ferromagnetism in these compounds.

In recent years, mixed solid solutions of the following systems have been studied intensively:<sup>[137-139]</sup>



It has been established that some alloys of these systems exhibit simultaneously ferromagnetism and superconductivity at very low temperatures. Such substances have attracted much attention. In the case of the first system,  $(CeGd)Ru_2$ , the curves of the transition points of the alloys from the superconducting to normal state ( $T_S$ ) and of the ferromagnetic Curie points ( $\theta$ ) intersect at  $\approx 6$  mol.%  $GdRu_2$  (Fig. 51). Thus, there is a region of compositions where the Curie point  $\theta$  is higher than  $T_S$ . If one of such solid solutions (for example,  $Ce_{0.95}Gd_{0.05}Ru_2$ ) is cooled below  $T_S$ , we can observe in it the superconducting and ferromagnetic states simultaneously. Such alloys were also found in the mixed solid solutions  $(YGd)Os_2$  and in the  $(CePr)Ru_2$  system. Owing to the existence of diamagnetic screening in superconductors, the magnetization and hysteresis curves of superconducting ferromagnets will be distorted. This may be explained as follows. In the superconducting state, the magnetic flux is forced out of the super-

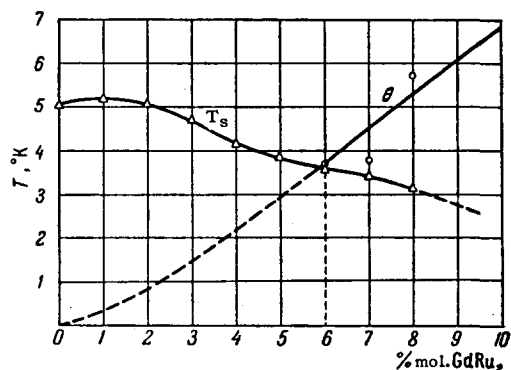


FIG. 51. Dependence of the Curie temperature  $\theta$  and the superconducting transition temperature  $T_S$  on the composition of the  $CeRu_2-GdRu_2$  system.

conductor, i.e., the induction is zero,

$$B = H + 4\pi I = 0. \quad (34)$$

Hence, we find that the magnetization is

$$I = -\frac{H}{4\pi}, \quad (35)$$

i.e., the characteristic diamagnetism of superconductors appears. Thus, in a sample exhibiting ferromagnetism and superconductivity simultaneously, when the field is increased a negative component of the magnetization appears in addition to the ferromagnetic magnetization. This phenomenon was observed<sup>[140,141]</sup> in measurements of the magnetic hysteresis loops at  $T = 1.3^\circ\text{K}$  in alloys of the  $(\text{CeGd})\text{Ru}_2$  system (Fig. 52).

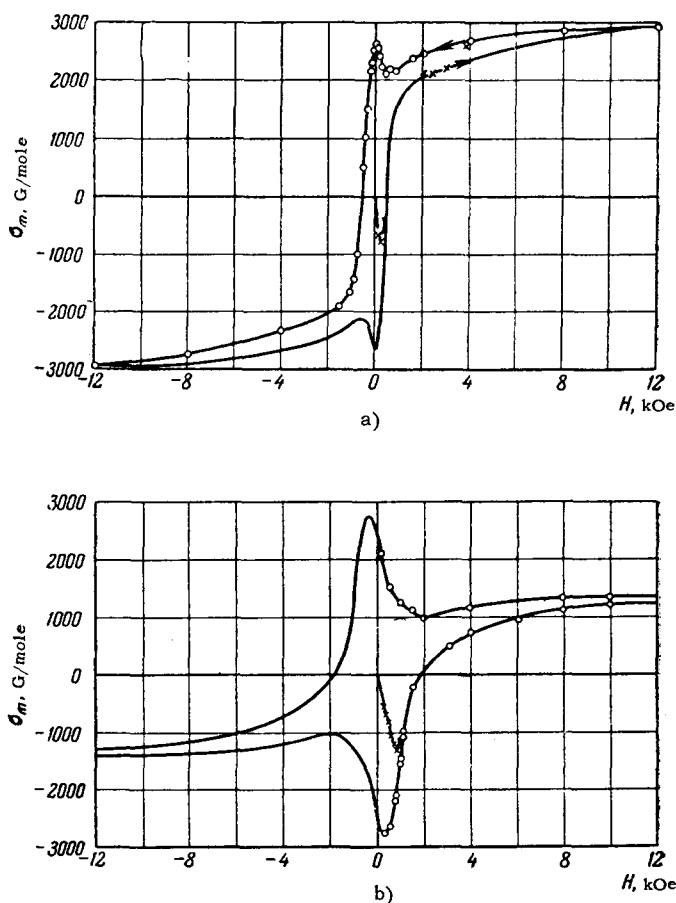


FIG. 52. Hysteresis loops at  $1.38^\circ\text{K}$  for the solutions: a) 8%  $\text{GdRu}_2$  in  $\text{CeRu}_2$ ; b) 4%  $\text{GdRu}_2$  in  $\text{CeRu}_2$ .

The distortion of the hysteresis loops consists of a downward bending of the branch of the loop in weak fields due to the superposition of the negative magnetization component. The magnetization is reduced only in magnetic fields below the critical field  $H_{\text{cr}}$ . On reaching  $H_{\text{cr}}$ , the superconductivity is destroyed and the hysteresis loop assumes its normal shape.

The interest in these alloys is due to the fact that for a long time superconductivity and ferromagnetism

were regarded as incompatible because of the Meissner effect: the destruction of the superconducting state either by an external magnetic field or by an internal effective field in a ferromagnet.

Several theoretical papers<sup>[142,143]</sup> have dealt with the microscopic mechanisms preventing the simultaneous existence of the ferromagnetic and superconducting states of matter. Therefore, to explain the properties of the alloys referred to above, it was suggested<sup>[144]</sup> that the sample consists of alternate superconducting and ferromagnetic layers so that the two states do not coexist in the same layer. Recent theoretical work<sup>[145-147]</sup> has shown, that, in certain cases, the coexistence of the superconductivity and ferromagnetism or antiferromagnetism is possible in the same region of a crystal.

2. Solid Solutions of Rare-Earth Metals in One Another and in Yttrium. Yttrium has the same crystal structure as gadolinium and a similar atomic volume. Therefore, these metals can form continuous solid solutions of substitution in a wide range of concentrations. Thoburn, Legvold, and Spedding<sup>[148]</sup> investigated the temperature dependence of the magnetization of yttrium-gadolinium alloys. In alloys containing less than 60% gadolinium, anomalies were detected in the temperature dependence of the magnetization, on the basis of which it was assumed that they exhibit two magnetic transitions: from the ferromagnetic to antiferromagnetic state (point  $\theta_1$ ) and from the antiferromagnetic to paramagnetic state (point  $\theta_2$ ). In the temperature range from  $\theta_1$  to  $\theta_2$ , the antiferromagnetism was relatively easily "destroyed" by a magnetic field. Therefore, the temperature dependence of the magnetization of these alloys varies strongly with the field used to measure these dependences (Fig. 53). The temperatures of the transitions  $\theta_1$  and  $\theta_2$  decrease on increase of the yttrium content. The same workers measured the effective atomic magnetic moments of the alloys. It was found that the presence of paramagnetic yttrium in an alloy increases somewhat the magnetic moment of the gadolinium atom compared with its moment in the pure metal. This fact is of great interest and apparently indicates that rare-earth metal atoms may polarize the shells of the nonmagnetic yttrium atoms.

According to Thoburn, Legvold, and Spedding,<sup>[108]</sup> all the alloys containing more than 60% gadolinium are "normal" ferromagnets, i.e., they do not exhibit magnetic anomalies near the temperature  $\theta_1$ .

However, later measurements\* showed that these alloys also have anomalies in the temperature dependence of the magnetic properties in weak fields in the temperature range next to the Curie point  $\theta_2$ .

At present, there is no direct confirmation of the existence of antiferromagnetism in Gd-Y alloys. The

\*These measurements were carried out by A. V. Ped'ko and L. I. Solntseva in our laboratory.

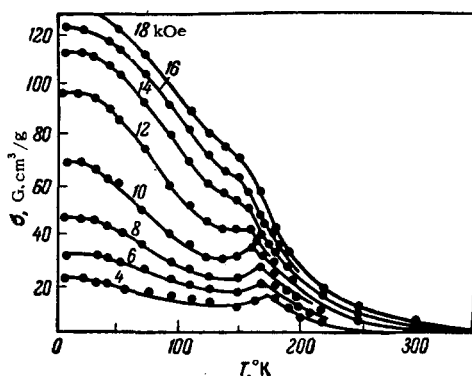


FIG. 53. Temperature dependence of the magnetization of the 50% Gd-50% Y alloy (in various fields).

position here is the same as for Gd.

Nelson and Legvold<sup>[150]</sup> studied single crystals of dilute solid solutions of gadolinium (1.0%), dysprosium (0.3 and 1%) and holmium (0.6 and 1.0%) in yttrium. In yttrium crystals with Gd and Dy (1% Dy) admixtures, the antiferromagnetic transition was found at 3.4° and 1.34°K, respectively. The remaining solutions were paramagnetic in the 1.2-4.2°K region, although the solution with Ho exhibited hysteresis of the magnetization curve. The antiferromagnetic ordering in dilute solutions of gadolinium and dysprosium in yttrium is apparently related to the indirect exchange between the solute atoms via the conduction electrons.

Thoburn, Legvold, and Spedding<sup>[148]</sup> reported data on the magnetic properties of gadolinium-lanthanum alloys. The alloy with 90% gadolinium was ferromagnetic, and the alloys with less gadolinium were antiferromagnetic. The temperatures of the transitions to the magnetically ordered state decreased on increase of the lanthanum content.

Our review shows that the magnetic behavior of rare-earth ferromagnets is more complicated than that of ferromagnets of the iron group. The mechanical application of the theories developed in the past to explain the behavior of the iron-group ferromagnets to r.e.f. is of limited use and in some cases it gives incorrect results. A theory of the exchange and magnetic interactions in r.e.f. should be based on the fundamental feature of the electron structure of rare-earth atoms, i.e., on the fact that their "magnetic" 4f-electrons lie deep in the electron shells. The mechanism of the exchange interaction between the 4f-electrons of neighboring atoms must necessarily be indirect. In recent years, several attempts have been made to develop a theory of indirect exchange in r.e.f. via the conduction electrons, as well as via the 5s<sup>2</sup> and 5p<sup>6</sup> electrons. These theories, however, are not yet perfect and they need further development.

Such development should naturally be accompanied by intensive and deeper experimental studies of the magnetic properties and electron structure of rare-earth metals, their alloys and compounds.

<sup>1</sup> F. Trombe, *Compt. rend.* 221, 19 (1945); 236, 591 (1953); *J. phys. radium* 12, 222 (1951).

<sup>2</sup> Elliott, Legvold, and Spedding, *Phys. Rev.* 94, 1143 (1954).

<sup>3</sup> Behrendt, Legvold, and Spedding, *Phys. Rev.* 109, 1544 (1958).

<sup>4</sup> S. Legvold, *Coll. Rare Earth Research*, Macmillan Company, N.Y. 1961, p. 142.

<sup>5</sup> Rhodes, Legvold, and Spedding, *Phys. Rev.* 109, 1547 (1958).

<sup>6</sup> Elliott, Legvold, and Spedding, *Phys. Rev.* 100, 1594 (1955).

<sup>7</sup> Green, Legvold, and Spedding, *Phys. Rev.* 122, 827 (1961).

<sup>8</sup> H. Leipfinger, *Z. Physik* 150, 415 (1958).

<sup>9</sup> Thoburn, Legvold, and Spedding, *Phys. Rev.* 112, 56 (1958).

<sup>10</sup> D. Davis and R. Bozorth, *Phys. Rev.* 118, 1543 (1960).

<sup>11</sup> Legvold, Spedding, Barson, and Elliott, *Revs. Modern Phys.* 25, 129 (1953).

<sup>12</sup> Elliott, Legvold, and Spedding, *Phys. Rev.* 91, 28 (1953).

<sup>13</sup> Belov, Levitin, Nikitin, and Ped'ko, *JETP* 40, 1562 (1961), *Soviet Phys. JETP* 13, 1096 (1961).

<sup>14</sup> K. P. Belov and A. V. Ped'ko, *JETP* 42, 87 (1962), *Soviet Phys. JETP* 15, 62 (1962).

<sup>15</sup> W. Henry, *J. Appl. Phys.* 31, 323S (1960).

<sup>16</sup> W. Henry, *J. Appl. Phys.* 30, 99S (1959).

<sup>17</sup> W. Henry, *J. phys. radium* 20, 192 (1959).

<sup>18</sup> W. Henry, *Phys. Rev.* 117, 89 (1960).

<sup>19</sup> W. Henry, *J. Appl. Phys.* 29, 524 (1958).

<sup>20</sup> V. Henry, *Coll. High Magnetic Fields*, John Wiley, N.Y., 1962, p. 522.

<sup>21</sup> Strandburg, Legvold, and Spedding, *Phys. Rev.* 127, 2046 (1962).

<sup>22</sup> K. P. Belov and S. A. Nikitin, *FMM* 13, 43 (1962).

<sup>23</sup> C. Graham, *J. Phys. Soc. Japan* 17, 1310 (1962).

<sup>24</sup> Corner, Roe, and Tayler, *Proc. Phys. Soc. (London)* 80, 927 (1962).

<sup>25</sup> L. D. Landau, *Phys. Z. der Sowjetunion (London)* 4, 675 (1933).

<sup>26</sup> S. A. Nikitin, *FMM* 15, 187 (1963).

<sup>27</sup> L. Bates and A. Pacey, *Proc. Phys. Soc. (London)* 78, 878 (1961).

<sup>28</sup> Telesnin, Al'meneva, and Pogozeva, *FTT* 4, 357 (1962), *Soviet Phys. Solid State* 4, 256 (1962).

<sup>29</sup> Wilkinson, Koehler, Cable, and Wollan, *J. Appl. Phys.* 31, 49S (1961).

<sup>30</sup> Koehler, Wollan, Wilkinson, and Cable, *Coll. Rare Earth Research*, Macmillan, N.Y., 1961, p. 149.

<sup>31</sup> W. Koehler, *J. Appl. Phys.* 31, 20S (1961).

<sup>32</sup> Koehler, Cable, and Wollan, *J. Phys. Soc. Japan* 17, 32S (1962).

<sup>33</sup> W. Koehler and E. Wollan, *Phys. Rev.* 97, 1177 (1955); Cable, Wollan, Koehler, and Wilkinson, *J. Appl. Phys.* 31, 48S (1961).

- <sup>34</sup> Koehler, Cable, Wollan, and Wilkinson, *J. Appl. Phys.* **33**, 1029S (1962); *Phys. Rev.* **126**, 1672 (1962).
- <sup>35</sup> A. Meyer and R. Tagland, *J. Phys. radium* **17**, 457 (1956).
- <sup>36</sup> A. Herpin and P. Meriel, *J. phys. radium* **22**, 337 (1961).
- <sup>37</sup> A. Yoshimori, *J. Phys. Soc. Japan* **14**, 807 (1952).
- <sup>38</sup> Biersted, Darnell, Cloud, Flippen, and Jarrett, *Phys. Rev. Letters* **8**, 15 (1962).
- <sup>39</sup> Herpin, Koehler, and Meriel, *Bull. Amer. Phys. Soc., Ser. II*, **5**, 457 (1960).
- <sup>40</sup> J. Hastings and L. Corless, *Phys. Rev.* **126**, 556 (1962).
- <sup>41</sup> Cable, Wilkinson, Wollan, and Koehler, *Phys. Rev.* **125**, 1860 (1962).
- <sup>42</sup> Bykov, Golovin, Ageev, Levik, and Vinogradov, *DAN SSSR* **128**, 1153 (1959), *Soviet Phys. Doklady* **4**, 1070 (1960); Kostina, Kozlova, and Kondorskiĭ, *JETP* **45**, 1352 (1963), *Soviet Phys. JETP* **18**, 931 (1964).
- <sup>43</sup> T. Kaplan, *Phys. Rev.* **116**, 888 (1959).
- <sup>44</sup> V. E. Naĭsh, Dissertation, Sverdlovsk, 1962.
- <sup>45</sup> L. Néel, *Compt. rend.* **242**, 1549, 1824 (1956); *Izv. AN SSSR, ser. fiz.* **21**, 901 (1957).
- <sup>46</sup> P. de Gennes, *J. phys. radium* **23**, 510 (1962).
- <sup>47</sup> B. Cooper, *Phys. Rev.* **118**, 135 (1960).
- <sup>48</sup> J. Villain, *J. Phys. Chem. Solids* **11**, 303 (1959).
- <sup>49</sup> T. Kaplan and D. Lyons, *Phys. Rev.* **129**, 2073 (1963).
- <sup>50</sup> Kaplan, Dright, Lyons, and Menyok, *J. Appl. Phys.* **32**, 13S (1961).
- <sup>51</sup> K. Yosida and H. Miwa, *J. Appl. Phys.* **32**, 8S (1961).
- <sup>52</sup> K. Yosida and H. Miwa, *Progr. Theoret. Phys. (Kyoto)* **26**, 693 (1961).
- <sup>53</sup> T. Kaplan, *Phys. Rev.* **124**, 329 (1961).
- <sup>54</sup> J. Elliott, *Phys. Rev.* **124**, 346 (1961); *J. Phys. Soc. Japan* **17**, Suppl. **B1**, 1 (1962).
- <sup>55</sup> A. Herpin, *J. phys. radium* **23**, 453 (1962).
- <sup>56</sup> T. Nagamiya, *J. Appl. Phys.* **33**, 1029S (1962). Nagamiya, Nagato, and Kitano, *Progr. Theoret. Phys. (Kyoto)* **27**, 1253 (1962); *J. Phys. Soc. Japan* **17**, Suppl. **B1**, 10 (1962).
- <sup>57</sup> H. Sato, *J. Phys. Chem. Solids* **19**, 541 (1961); *J. Appl. Phys.* **32**, 53S (1961).
- <sup>58</sup> Liu, Behrendt, Legvold, and Good, *Phys. Rev.* **116**, 1464 (1959).
- <sup>59</sup> U. Enz, *Physica* **26**, 698 (1960); *J. Appl. Phys.* **32**, 22S (1961).
- <sup>60</sup> C. Kittel, *Phys. Rev.* **120**, 335 (1960).
- <sup>61</sup> Herpin, Meriel, and Villain, *Compt. rend.* **249**, 1334 (1959); *J. phys. radium* **21**, 67 (1960); A. Herpin and P. Meriel, *Compt. rend.* **250**, 1450 (1960).
- <sup>62</sup> R. Bozorth and D. Davis, *J. Phys. Soc. Japan* **17**, 112S (1962).
- <sup>63</sup> C. Been and D. Rodbell, *Phys. Rev.* **126**, 104 (1962).
- <sup>64</sup> Banister, Legvold, and Spedding, *Phys. Rev.* **94**, 1140 (1954).
- <sup>65</sup> Griffel, Skochdopole, and Spedding, *J. Chem. Phys.* **25**, 75 (1956).
- <sup>66</sup> Gerstein, Griffel, Jennings, Miller, Skochdopole, and Spedding, *J. Chem. Phys.* **27**, 394 (1957).
- <sup>67</sup> R. Skochdopole, *J. Chem. Phys.* **23**, 2258 (1955).
- <sup>68</sup> Griffel, Skochdopole, and Spedding, *Phys. Rev.* **93**, 657 (1954).
- <sup>69</sup> Jennings, Stanton, and Spedding, *J. Chem. Phys.* **27**, 909 (1957).
- <sup>70</sup> Jennings, Hill, and Spedding, *J. Chem. Phys.* **34**, 2082 (1961).
- <sup>71</sup> K. P. Belov, *Magnitnye prevrashcheniya (Magnetic Transformations)*, M., Fizmatgiz, 1959.
- <sup>72</sup> J. Lock, *Proc. Phys. Soc. (London)* **B70**, 566 (1957).
- <sup>73</sup> C. McHargue and H. Vakel, *Acta Met.* **8**, 637 (1960).
- <sup>74</sup> Wilkinson, Child, McHargue, Koehler, and Wollan, *Phys. Rev.* **122**, 1409 (1961).
- <sup>75</sup> C. La Blanchetais, *Compt. rend.* **220**, 392 (1945).
- <sup>76</sup> Parkinson, Simon, and Spedding, *Proc. Roy. Soc. (London)* **A207**, 139 (1951).
- <sup>77</sup> D. Parkinson and L. Roberts, *Proc. Phys. Soc. (London)* **B70**, 471 (1957).
- <sup>78</sup> James, Legvold, and Spedding, *Phys. Rev.* **88**, 1092 (1952).
- <sup>79</sup> E. Itskevich, *JETP* **42**, 1173 (1962), *Soviet Phys. JETP* **15**, 811 (1962).
- <sup>80</sup> P. Graf, *Z. angew. Phys.* **13**, 534 (1961).
- <sup>81</sup> Alstad, Colvin, Legvold, and Spedding, *Phys. Rev.* **121**, 1637 (1961).
- <sup>82</sup> Behrendt, Legvold, and Spedding, *Phys. Rev.* **106**, 723 (1957).
- <sup>83</sup> L. Roberts, *Proc. Phys. Soc. (London)* **B70**, 434 (1957).
- <sup>84</sup> Jennings, Hill, and Spedding, *J. Chem. Phys.* **31**, 1240 (1959).
- <sup>85</sup> C. La Blanchetais and F. Trombe, *Compt. rend.* **243**, 707 (1956); W. Klemm and H. Bommer, *Z. anorg. u. allgem. Chem.* **231**, 138 (1937).
- <sup>86</sup> R. Bozorth and J. Van Vleck, *Phys. Rev.* **118**, 1493 (1960).
- <sup>87</sup> Curry, Legvold, and Spedding, *Phys. Rev.* **117**, 953 (1960).
- <sup>88</sup> Olsen, Neresen, and Arnold, *J. Appl. Phys.* **33**, 1135S (1962).
- <sup>89</sup> P. Z. Levitin and S. A. Nikitin, *FMM* **2**, 948 (1961).
- <sup>90</sup> E. Lee and L. Alberts, *Proc. Phys. Soc. (London)* **79**, 997 (1962).
- <sup>91</sup> S. Legvold, *Abstracts of a Symposium on Ferromagnetism and Ferroelectricity*, Leningrad, U.S.S.R. Academy of Sciences Press, 1963.
- <sup>92</sup> Belov, Levitin, and Nikitin, *Izv. AN SSSR, ser. fiz.* **25**, 1382 (1961), *Columbia Tech. Transl.* **25**, 1394 (1961).
- <sup>93</sup> S. A. Nikitin, *JETP* **43**, 31 (1962), *Soviet Phys. JETP* **16**, 21 (1963).
- <sup>94</sup> W. Corner and F. Hutchinson, *Proc. Phys. Soc. (London)* **75**, 781 (1960).

- <sup>95</sup> K. P. Belov and S. A. Nikitin, *JETP* **42**, 403 (1962), *Soviet Phys. JETP* **15**, 279 (1962).
- <sup>96</sup> R. Bozorth and T. Wakiyama, *J. Phys. Soc. Japan* **18**, 97 (1963).
- <sup>97</sup> W. Mason, *Phys. Rev.* **96**, 302 (1954).
- <sup>98</sup> F. Darnell and E. Moore, *J. Appl. Phys.* **94**, 1335 (1963).
- <sup>99</sup> Belov, Levitin, Malevskaya, and Sokolov, *FMM* **16**, No. 3 (1964).
- <sup>100</sup> Belov, Nikitin, and Ped'ko, *JETP* **45**, 26 (1963), *Soviet Phys. JETP* **18**, 20 (1964).
- <sup>101</sup> S. Liu, *Phys. Rev.* **127**, 1889 (1962).
- <sup>102</sup> Colvin, Legvold, and Spedding, *Phys. Rev.* **120**, 741 (1960).
- <sup>103</sup> Hall, Legvold, and Spedding, *Phys. Rev.* **117**, 971 (1960).
- <sup>104</sup> P. Bridgman, *Proc. Amer. Acad. Arts Sci.* **83**, 1 (1954).
- <sup>105</sup> R. R. Birss and S. Day, *Proc. Roy. Soc. (London)* **A263**, 474 (1961).
- <sup>106</sup> N. V. Vol'kenshtein and G. F. Fedorov, *JETP* **44**, 825 (1963), *Soviet Phys. JETP* **17**, 560 (1963).
- <sup>107</sup> T. Kasya, *Progr. Theoret. Phys. (Kyoto)* **16**, 58 (1956).
- <sup>108</sup> P. de Gennes and J. Freidel, *J. Phys. Chem. Solids* **4**, 71 (1958).
- <sup>109</sup> R. Brout and H. H. Suhl, *Phys. Rev. Letters* **2**, 367 (1959).
- <sup>110</sup> Yu. L. Irkhin, *FMM* **6**, 214 (1958).
- <sup>111</sup> E. A. Turov and Yu. L. Irkhin, *FMM* **9**, 488 (1960).
- <sup>112</sup> H. Miwa, *Progr. Theoret. Phys. (Kyoto)* **28**, 208 (1962).
- <sup>113</sup> A. Macintosh, *Phys. Rev. Letters* **9**, 90 (1962).
- <sup>114</sup> Born, Legvold, and Spedding, *J. Appl. Phys.* **32**, 2543 (1961).
- <sup>115</sup> A. V. Ped'ko, *Dissertation, Moscow State University*, 1962.
- <sup>116</sup> Kevane, Legvold, and Spedding, *Phys. Rev.* **91**, 1372 (1953).
- <sup>117</sup> Anderson, Legvold, and Spedding, *Phys. Rev.* **111**, 1257 (1958).
- <sup>118</sup> Vonsovskii, Kobelev, and Rodionov, *Izv. AN SSSR, ser. fiz.* **16**, 569 (1952).
- <sup>119</sup> R. Karplus and I. Luttinger, *Phys. Rev.* **95**, 1154 (1954).
- <sup>120</sup> N. V. Vol'kenshtein and G. V. Fedorov, *Izv. AN SSSR, ser. fiz.* **25**, 1379 (1961), *Columbia Tech. Transl.* **25**, 1391 (1961).
- <sup>121</sup> A. Marotta and K. Tauer, *J. Phys. Soc. Japan* **18**, 310 (1962).
- <sup>122</sup> Nesbitt, Williams, Wernick, and Sherwood, *J. Appl. Phys.* **33**, 1674 (1962).
- <sup>123</sup> L. Cherry and W. Wallace, *J. Appl. Phys.* **33**, 1515 (1962).
- <sup>124</sup> Vickery, Sexton, Navy, and Kleber, *J. Appl. Phys.* **31**, 366S (1960).
- <sup>125</sup> Nesbitt, Wernick, and Corenzwit, *J. Appl. Phys.* **30**, 365 (1959).
- <sup>126</sup> Nassau, Cherry, and Wallace, *J. Phys. Chem. Solids* **16**, 131 (1960).
- <sup>127</sup> Nesbitt, Williams, Wernick, and Sherwood, *J. Appl. Phys.* **32**, 342S (1961).
- <sup>128</sup> James, Lemare, and Bertaut, *Compt. rend.* **255**, 896 (1962).
- <sup>129</sup> Hubbard, Adams, and Gilerich, *J. Appl. Phys.* **31**, 368S (1961).
- <sup>130</sup> W. Hubbard and E. Adams, *J. Phys. Soc. Japan* **17**, Suppl. BI, 112 (1962).
- <sup>131</sup> V. I. Chechernikov, *FMM* **16**, 324 (1963).
- <sup>132</sup> L. Cherry and W. Wallace, *J. Appl. Phys.* **32**, 340S (1961).
- <sup>133</sup> Williams, Wernick, and Nesbitt, *Abstracts of a Conference on Magnetism, Kyoto, 1961*.
- <sup>134</sup> Jaccarino, Matthias, Peter, Suhl, and Wernick, *Phys. Rev. Letters* **5**, 251 (1960).
- <sup>135</sup> Matthias, Clogston, Williams, Corenzwit, and Sherwood, *Phys. Rev. Letters* **7**, 7 (1961).
- <sup>136</sup> Bozorth, Matthias, Suhl, and Corenzwit, *Phys. Rev.* **115**, 1595 (1959).
- <sup>137</sup> Matthias, Suhl, and Corenzwit, *Phys. Rev. Letters* **1**, 92 (1958).
- <sup>138</sup> Matthias, Compton, Suhl, and Corenzwit, *Phys. Rev.* **115**, 1597 (1959).
- <sup>139</sup> Hein, Falge, Matthias, and Corenzwit, *Phys. Rev. Letters* **2**, 500 (1959).
- <sup>140</sup> R. Bozorth and D. Davis, *J. Appl. Phys.* **31**, 321S (1960).
- <sup>141</sup> Bozorth, Matthias, Suhl, Corenzwit, and Davis, *Phys. Rev.* **115**, 1595 (1959).
- <sup>142</sup> V. M. Ginzburg, *JETP* **31**, 202 (1956), *Soviet Phys. JETP* **4**, 153 (1957).
- <sup>143</sup> S. V. Vonsovskii and M. A. Svirskii, *JETP* **40**, 1676 (1961), *Soviet Phys. JETP* **13**, 1182 (1961).
- <sup>144</sup> C. Herring and H. Suhl, *J. Appl. Phys.* **29**, 84S (1958).
- <sup>145</sup> A. I. Akhiezer and I. A. Akhiezer, *JETP* **43**, 2208 (1962), *Soviet Phys. JETP* **16**, 1560 (1963).
- <sup>146</sup> I. A. Pivovotskii, *JETP* **43**, 2255 (1962), *Soviet Phys. JETP* **16**, 1593 (1963).
- <sup>147</sup> S. V. Vonsovskii and M. A. Svirskii, *FMM* **15**, 316 (1963).
- <sup>148</sup> Thoburn, Legvold, and Spedding, *Phys. Rev.* **110**, 1298 (1958).
- <sup>149</sup> R. White, *J. Appl. Phys.* **32**, 1178 (1961). W. Wolf, *J. Appl. Phys.* **32**, 742 (1961).
- <sup>150</sup> D. Nelson and S. Legvold, *Phys. Rev.* **123**, 80 (1961).
- <sup>151</sup> E. Smidt and A. Daane, *J. Phys. Chem. Solids* **24**, 361 (1963).
- <sup>152</sup> C. D. Graham, *J. Appl. Phys.* **34**, 1341 (1963).
- <sup>153</sup> Nigh, Legvold, and Spedding, *Preprint, Inst. for Atomic Res., Iowa State University*.

Translated by A. Tybulewicz